Derisking Geological Storage w/ simulation-based seismic monitoring design & machine learning

Felix J. Herrmann[1,2,3]

[1]School of Electrical and Computer Engineering, Georgia Institute of Technology
[2]School of Earth and Atmospheric Sciences, Georgia Institute of Technology
[3]School of Computational Science and Engineering, Georgia Institute of Technology

SLIM

Georgia Institute of Technology

ML4Seismic

Georgia Tech College of Computing
School of Computational Science and Engineering

Georgia Tech College of Sciences
School of Earth and Atmospheric Sciences

Georgia Tech College of Engineering
School of Electrical and Computer Engineering

Derisking Geological Storage w/ simulation-based seismic monitoring design & machine learning

Huseyin Tuna Erdinc[1] , Abhinav Prakash Gahlot[2] , Ziyi Yin[3] , Mathias Louboutin[2] , Felix J. Herrmann[1,2,3]

[1]School of Electrical and Computer Engineering, Georgia Institute of Technology
[2]School of Earth and Atmospheric Sciences, Georgia Institute of Technology
[3]School of Computational Science and Engineering, Georgia Institute of Technology

SLIM
Georgia Institute of Technology

ML4Seismic

Georgia Tech College of Computing
School of Computational Science and Engineering

Georgia Tech College of Sciences
School of Earth and Atmospheric Sciences

Georgia Tech College of Engineering
School of Electrical and Computer Engineering

Wood et. al, Locked away – geological carbon storage, The Royal Society, October 2022
Ringrose, Philip. How to store CO2 underground: Insights from early-mover CCS Projects, 2020.

SLIM
ML4Seismic

Challenges

monitoring Geological CO_2 Storage in Saline Aquifers

Regulators & general public require transparency & assurances that *supercritical* CO_2 stays put in the *storage complex*

- *reservoir* simulations alone are *uncertain* due to large *variability* permeability
- risk profile storage & containment highest at start & at end
- there is a need for *reproducibility*

Develop low-cost time-lapse seismic system to monitor CO_2 plumes

- maximally captures information collected over many decades
- low-cost by being sparse w/o insisting on replication of surveys
- attains accuracy needed to detect early onset leakage *automatically*
- *collect 1–2* orders of magnitude *cheaper* over a *century*

Systematic assessment of risks using techniques from uncertainty quantification.

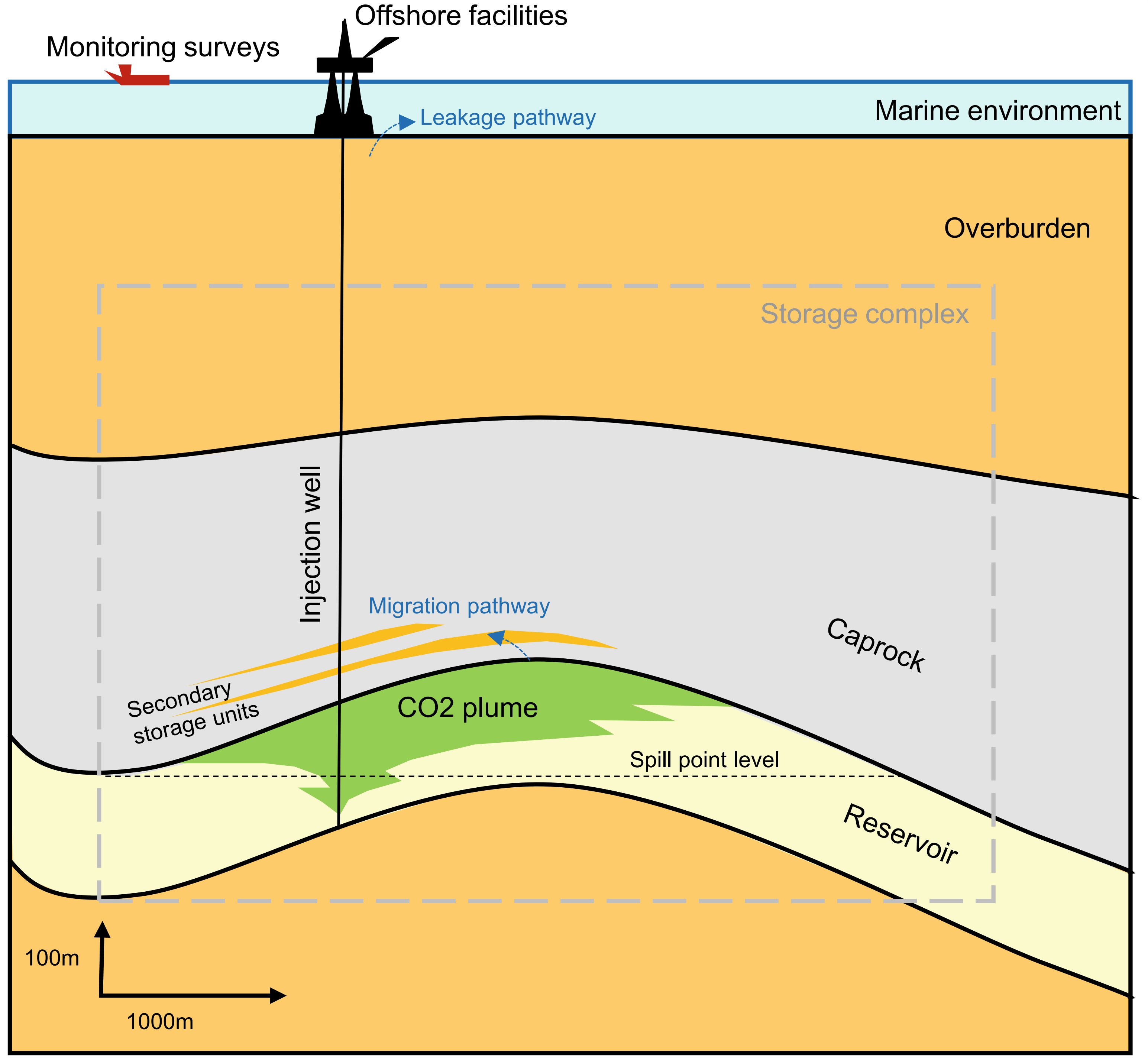

from Ringrose

UK Government publication “Deep Geological Storage of CO2 on the UK Continental Shelf: Containment Certainty”

Risk profiles

Uncertainties & risk *storage* model

- *highest* at *start*
- diminish when *more* time-lapse data is *collected*

***Containment* risk increases**

- w/ *amount* of CO_2 stored
- w/ size *area* undergoing *pressure* changes

There can be ***NO*** *lapse* in *monitoring* because

- any lack of *transparency* conformance
- will lead in loss in *confidence* by the *general* public

High-fidelity time-lapse information needs to be collected regularly over long periods of time!

uncertainty profile

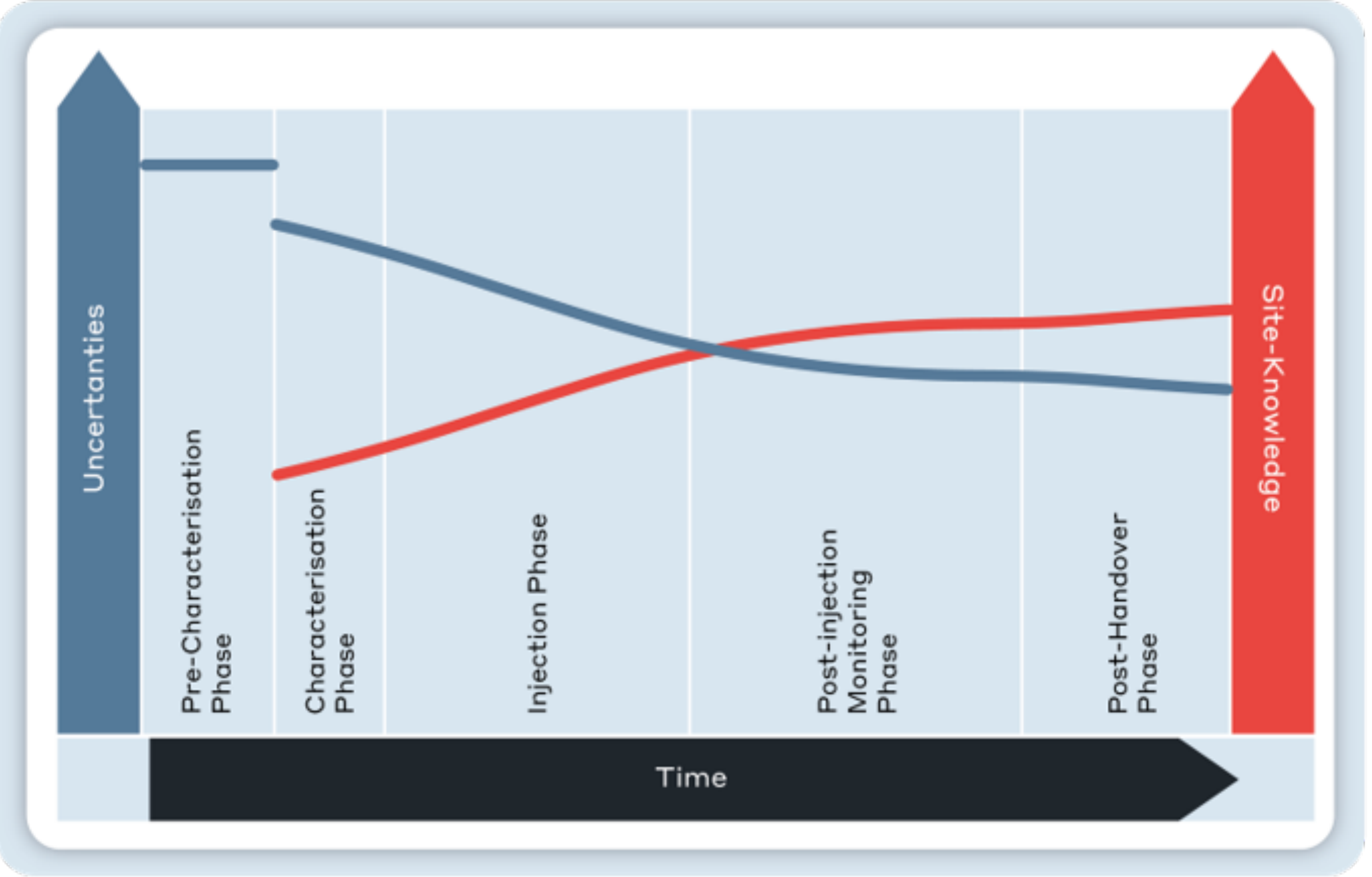

containment risk profile

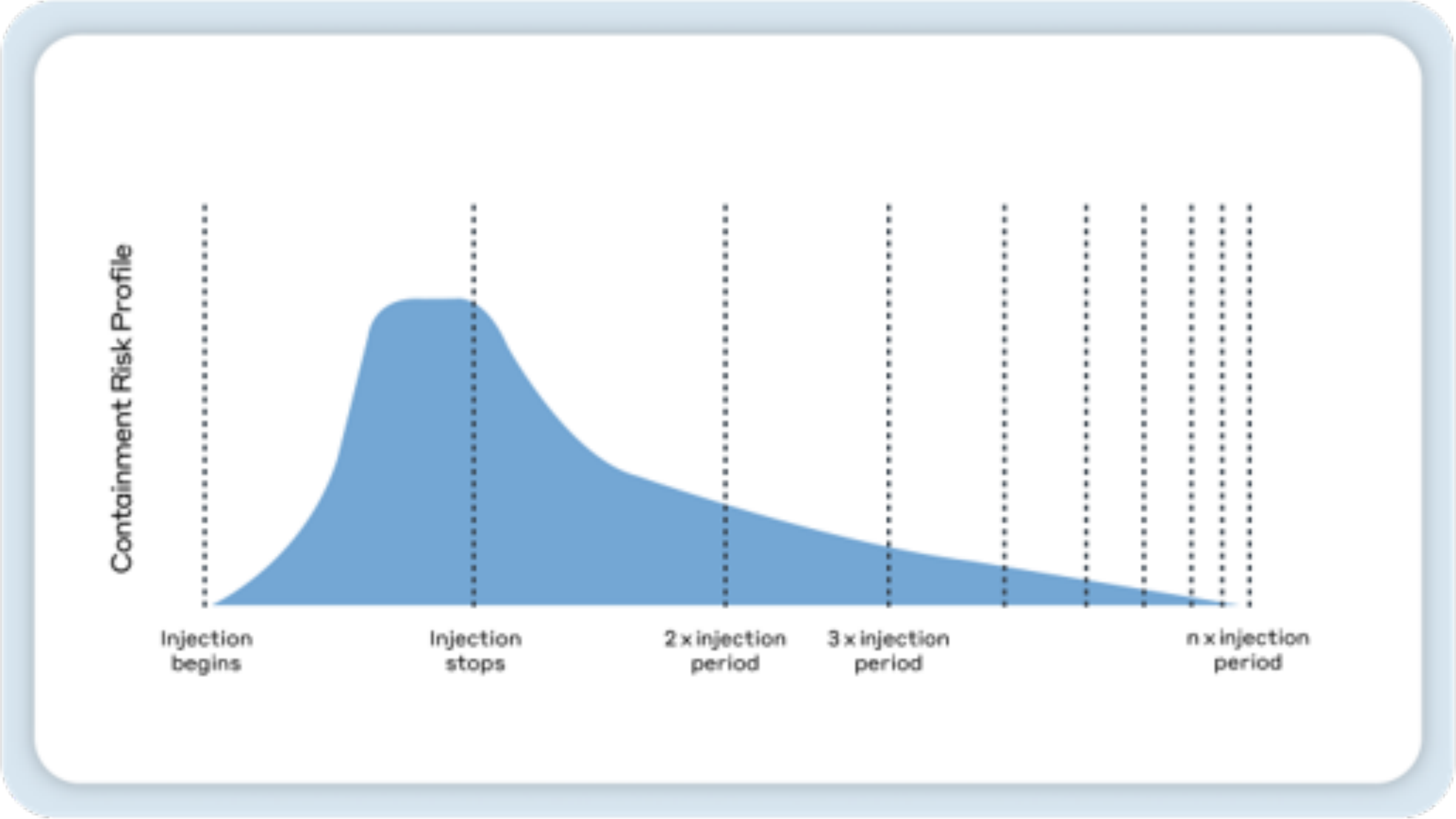

SLIM
ML4Seismic

Workflow simulation-based seismic monitoring design

Ziyi Yin, Huseyin Tuna Erdinc, Abhinav Prakash Gahlot, Mathias Louboutin and F. Herrmann. “Derisking geological carbon storage from high-resolution time-lapse seismic to explainable leakage detection.” The Leading Edge (2023).

Workflow

Ziyi Yin, Huseyin Tuna Erdinc, Abhinav Prakash Gahlot, Mathias Louboutin and F. Herrmann. “Derisking geological carbon storage from high-resolution time-lapse seismic to explainable leakage detection.” The Leading Edge (2023).

Rock property conversion

Workflow


proxy model
wavespeed, density
reservoir model
permeability, porosity
pressure induced fault
two-phase flow
CO2 dynamics
concentration, pressure
leakage
regular
time-lapse models
wavespeed, density
time-lapse (diff) data
time-lapse imaging
deep neural classifier
class activation mapping
leakage
regular
Confusion Matrix
True Neg
193
48.98%
False Pos
13
3.30%
False Neg
41
10.41%
True Pos
147
37.31%
No Leakage
Leakage
No Leakage
Leakage
accuracy = 86.29%

Conversion

velocity $\Longrightarrow$ permeability

Converted with v_p 1km/s $\uparrow \Rightarrow K$ 1.63mD $\uparrow$

- K permeability
- v_p compressional wavespeed

Three main geologic sections:

- secondary seal – Haisborough group (blue, > 300m, permeability $15 - 18$mD)
- primary seal – Rote Halite member (black, 50m, permeability $10^{-4} - 10^{-2}$mD)
- saline aquifer – Bunter sandstone (red, $300 - 500$m, permeability > 200mD)

Values taken from Strategic UK CCS Storage Appraisal Project

compressional wavespeed [km/s]

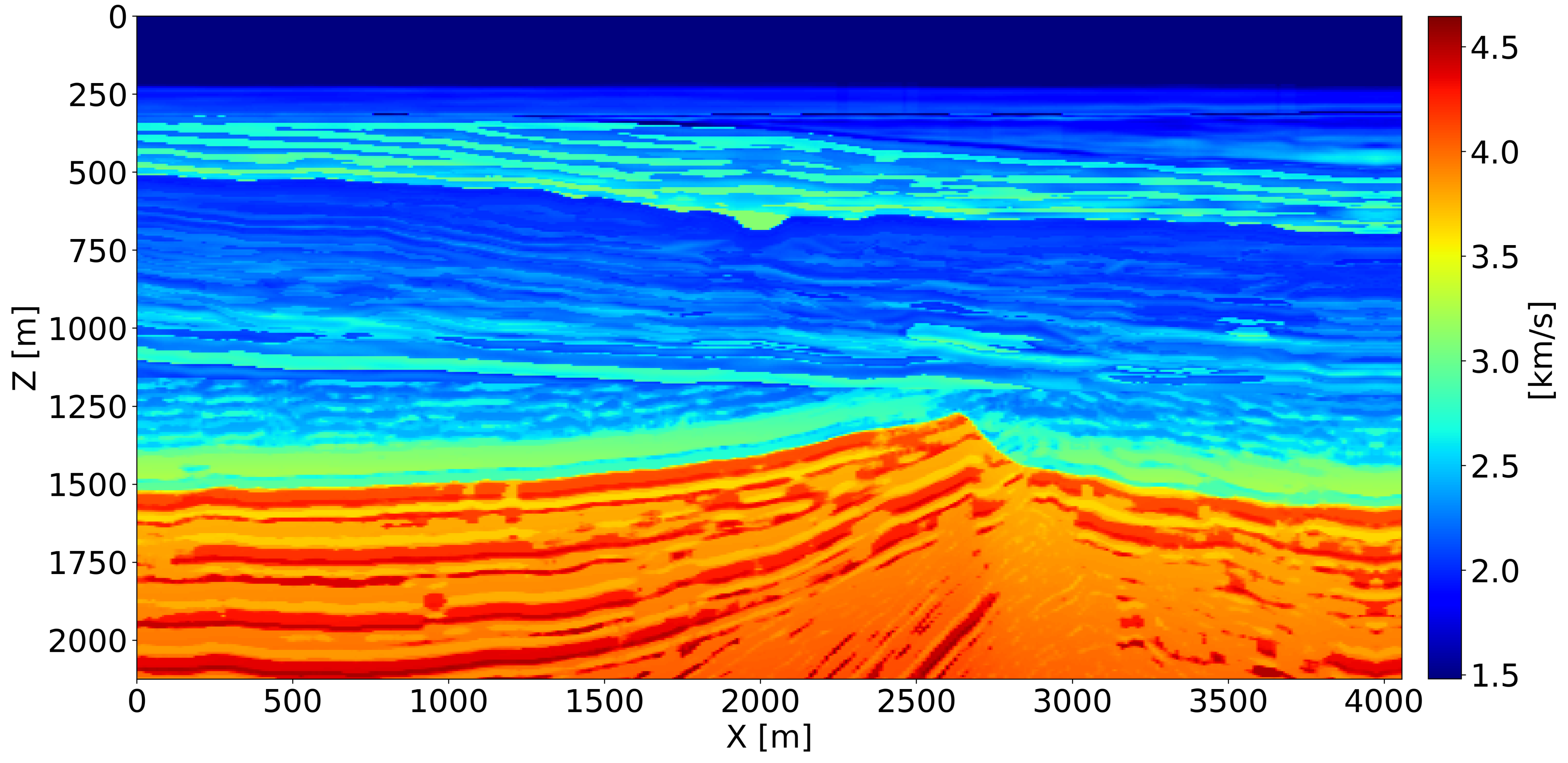

permeability [mD]

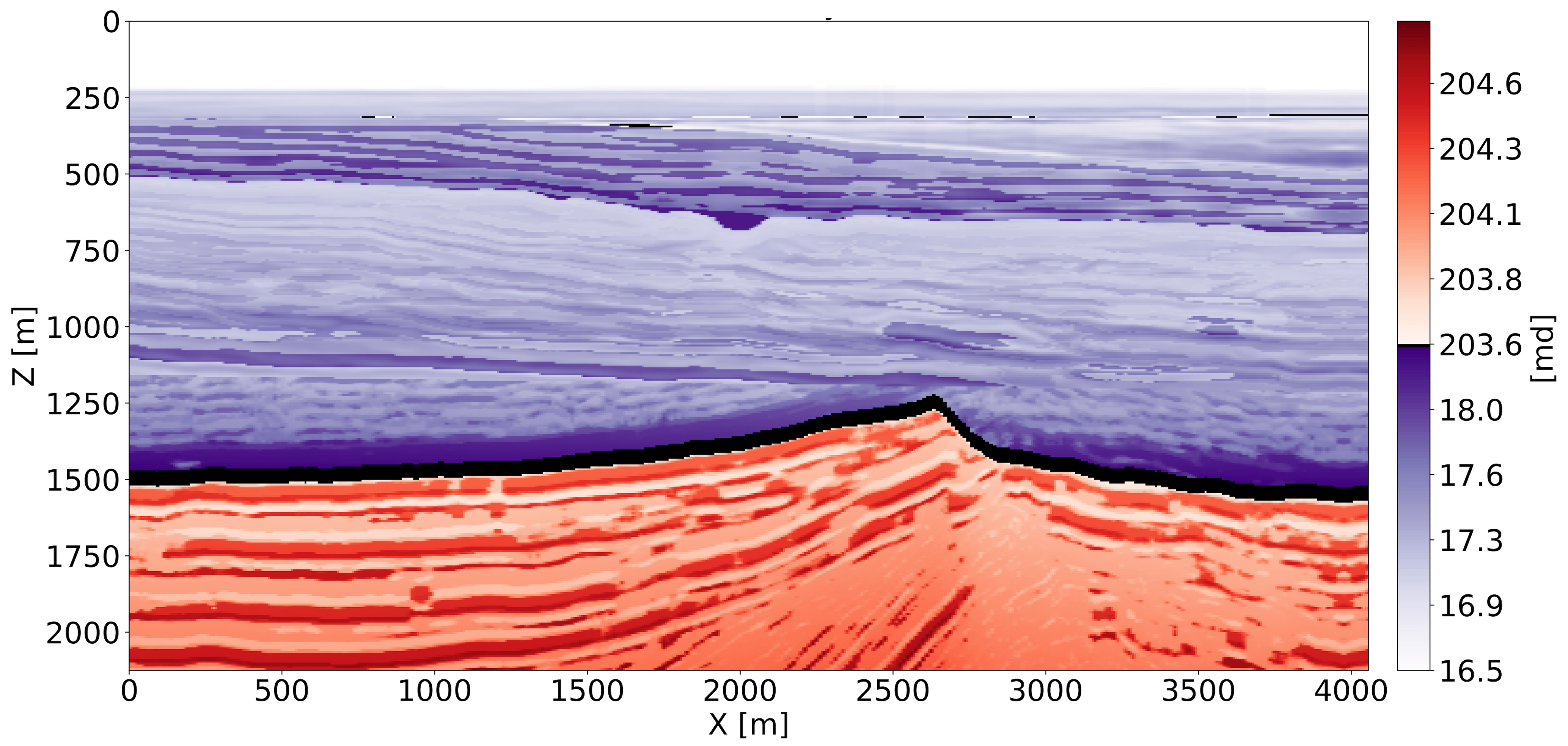

Costa, Antonio. "Permeability-porosity relationship: A reexamination of the Kozeny-Carman equation based on a fractal pore-space geometry assumption." Geophysical research letters 33.2 (2006).

Conversion

permeability $\Longrightarrow$ porosity

Kozeny-Carman relationship:

$$K = \phi^3 \left(\frac{1.527}{0.0314(1-\phi)} \right)^2$$

- K permeability
- ϕ porosity
- values taken from Strategic UK CCS Storage Appraisal Project

Permeability & porosity models serve as input for two-phase fluid flow simulations.

permeability [mD]

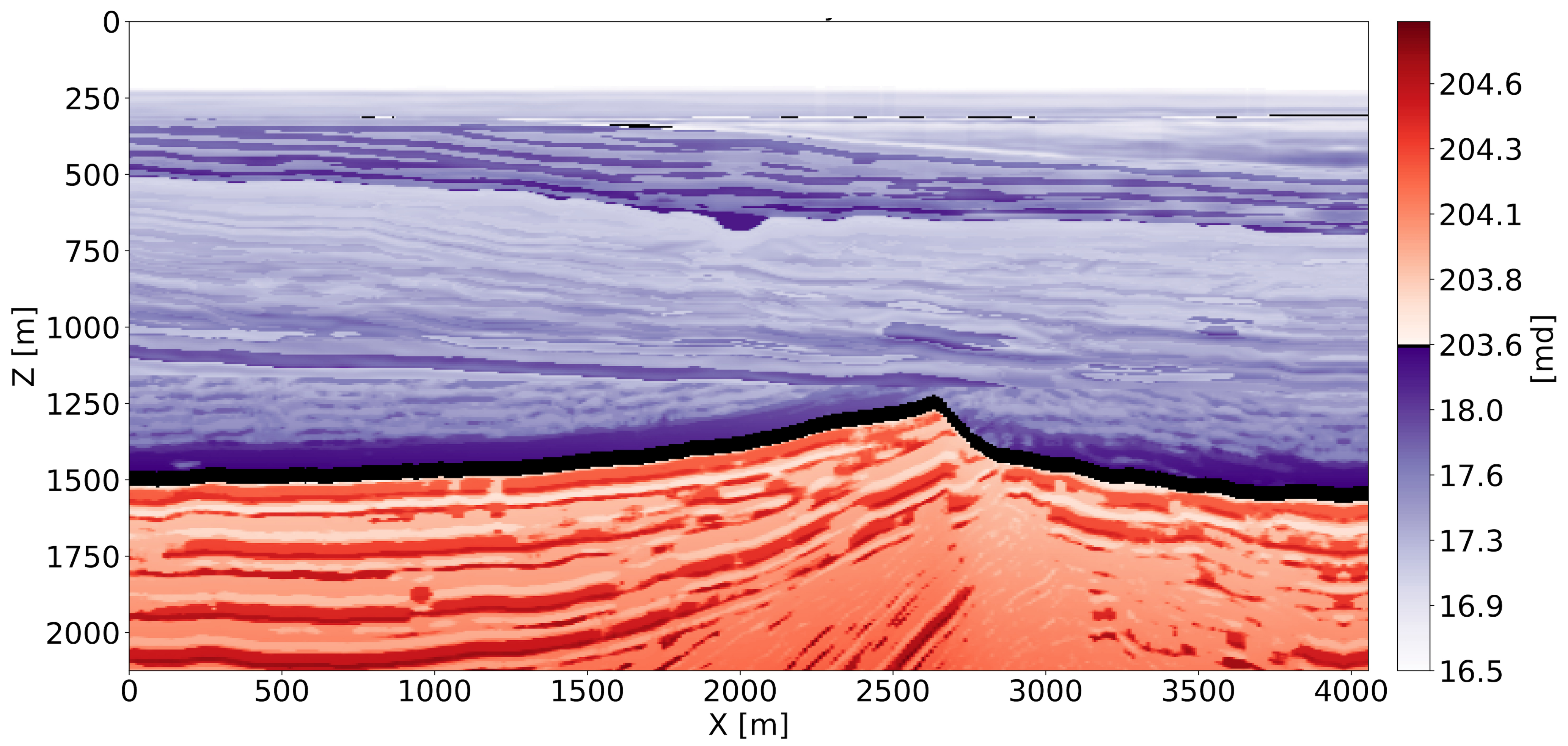

porosity [%]

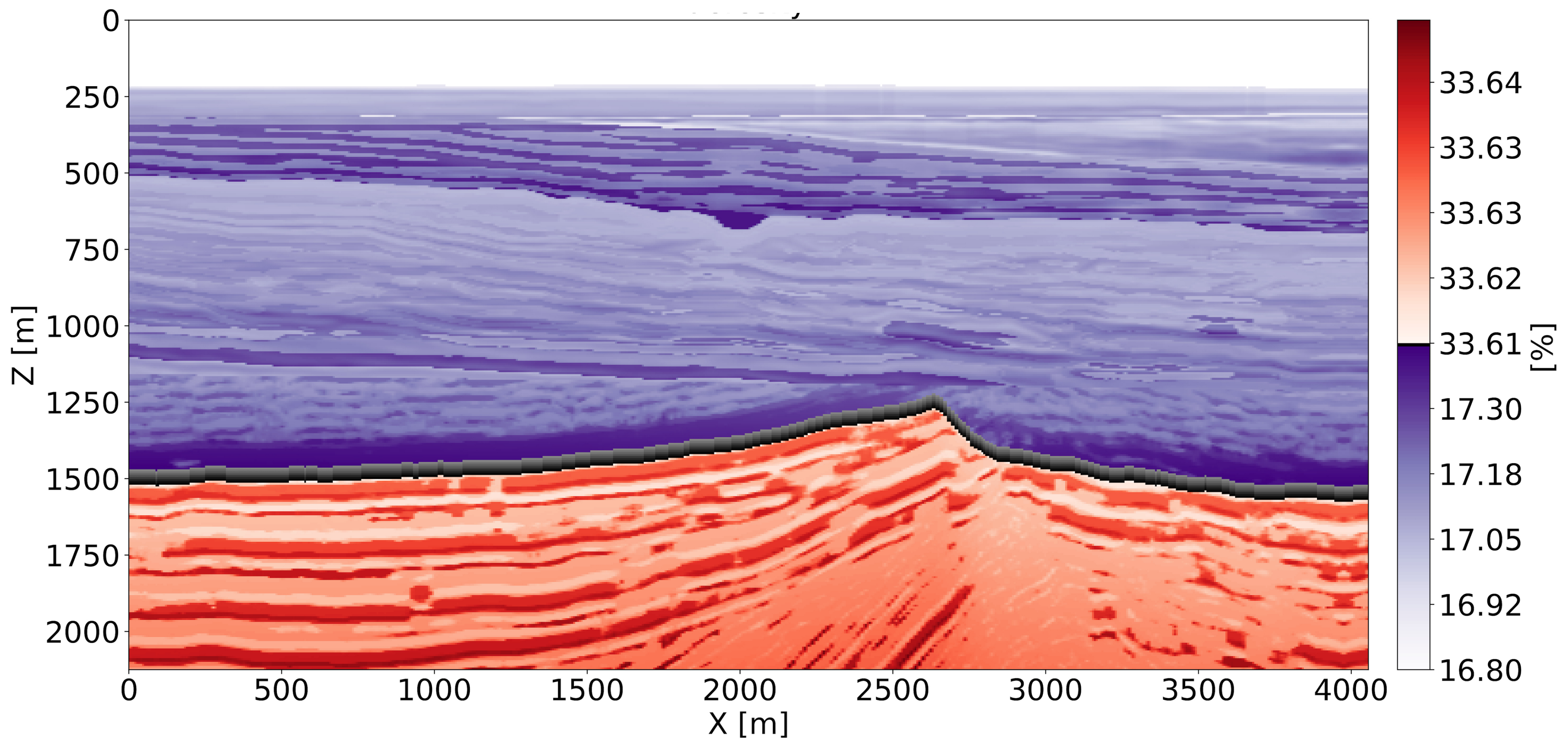

Fluid-flow modeling

Workflow


proxy model
wavespeed, density
reservoir model
permeability, porosity
pressure
induced
fault
two-phase
flow
CO2 dynamics
concentration, pressure
leakage
regular
time-lapse models
wavespeed, density
time-lapse (diff) data
time-lapse imaging
deep neural classifier
class activation mapping
leakage
regular
Confusion Matrix
No Leakage
Leakage
True Neg
193
48.98%
False Pos
13
3.30%
False Neg
41
10.41%
True Pos
147
37.31%
No Leakage
Leakage
accuracy = 86.29%

CO_2 dynamics

two-phase flow equations

mass balance equation:

$$\frac{\partial}{\partial t}(\phi S_i \rho_i) + \nabla \cdot (\rho_i \mathbf{v}_i) = \rho_i q_i, \quad i = 1,2$$

inject CO_2 to replace water

$$S_1 + S_2 = 1$$

Darcy's law:

$$\mathbf{v}_i = -\frac{K k_{ri}}{\tilde{\mu}_i}(\nabla P_i - g \rho_i \nabla Z), \quad i = 1,2$$

fluid pressure:

$$P_2 = P_1 - P_c(S_2)$$

Symbol	Meaning
K	permeability
ϕ	porosity
k_{ri}	relative permeability
S_i	fluid saturation
P_i	fluid pressure
P_c	capillary pressure
$\mathbf{v}_i$	Darcy's velocity
ρ_i	fluid density
$\tilde{\mu}_i$	fluid viscosity
q_i	injection/production rate
g	gravity constant
Z	vector of vertical direction

Pressure-induced fractures

Philip Ringrose. How to Store CO2 Underground: insights from early-mover CCS Projects. Springer, 2020. URL: https://link.springer.com/book/10.1007/978-3-030-33113-9.

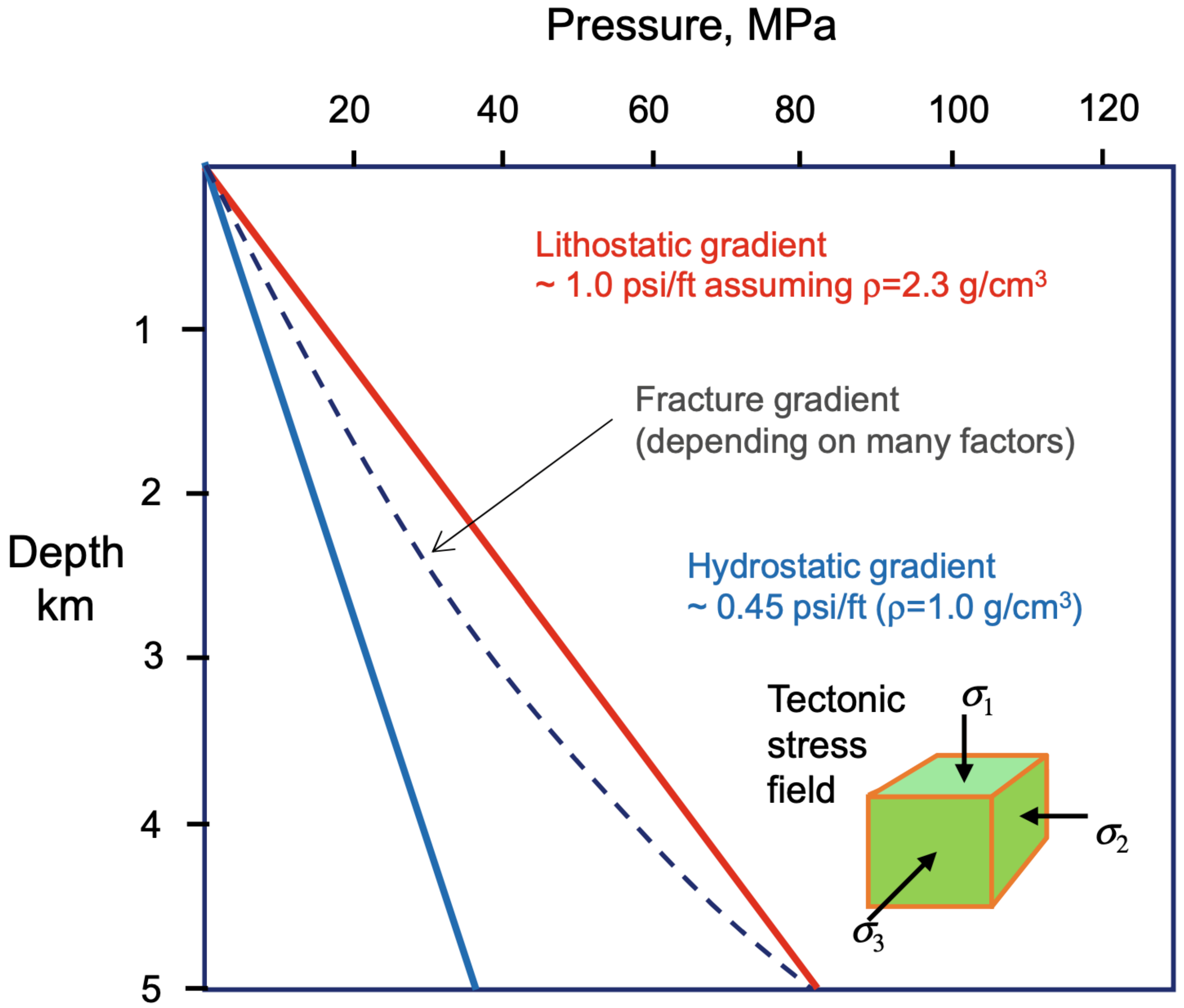

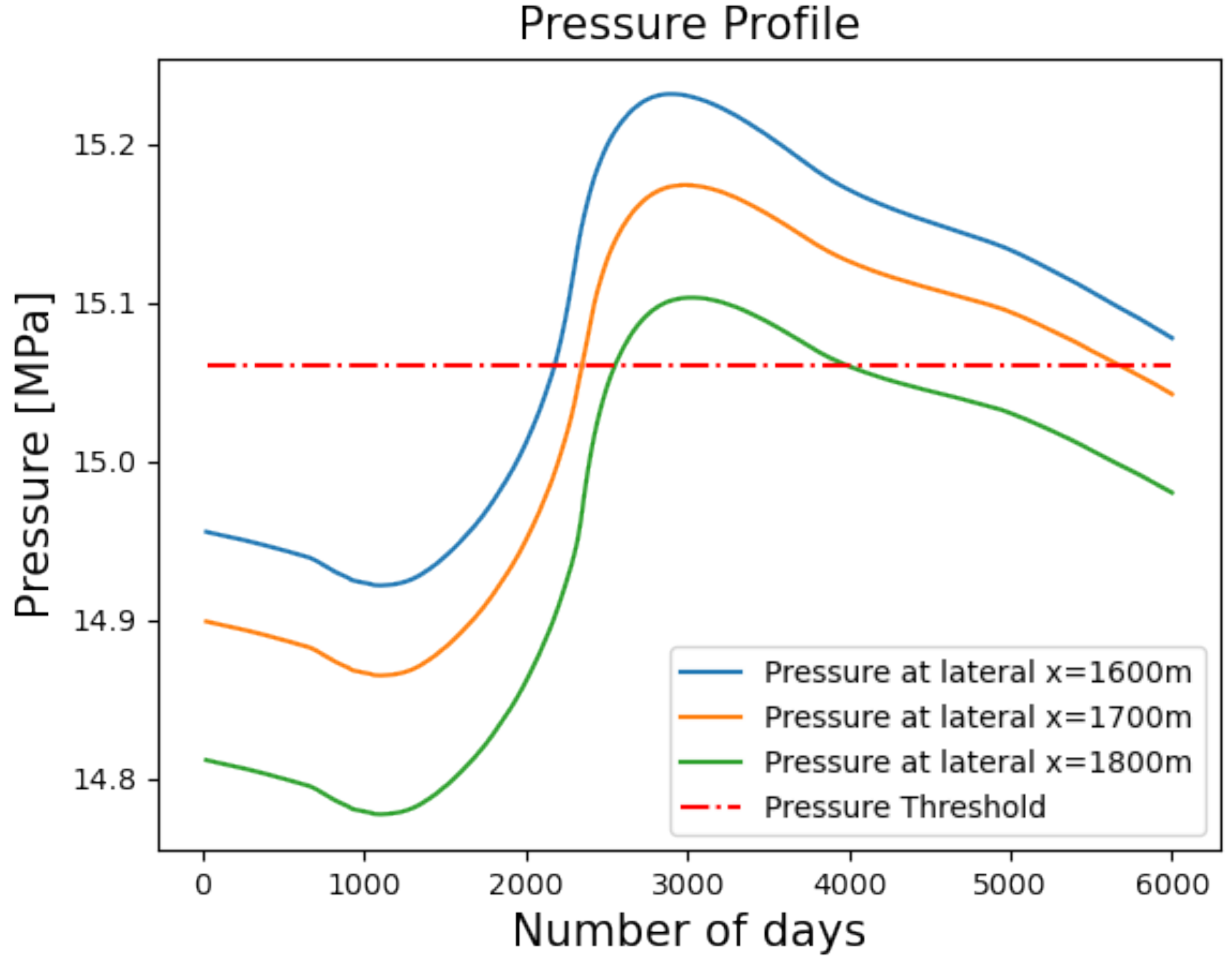

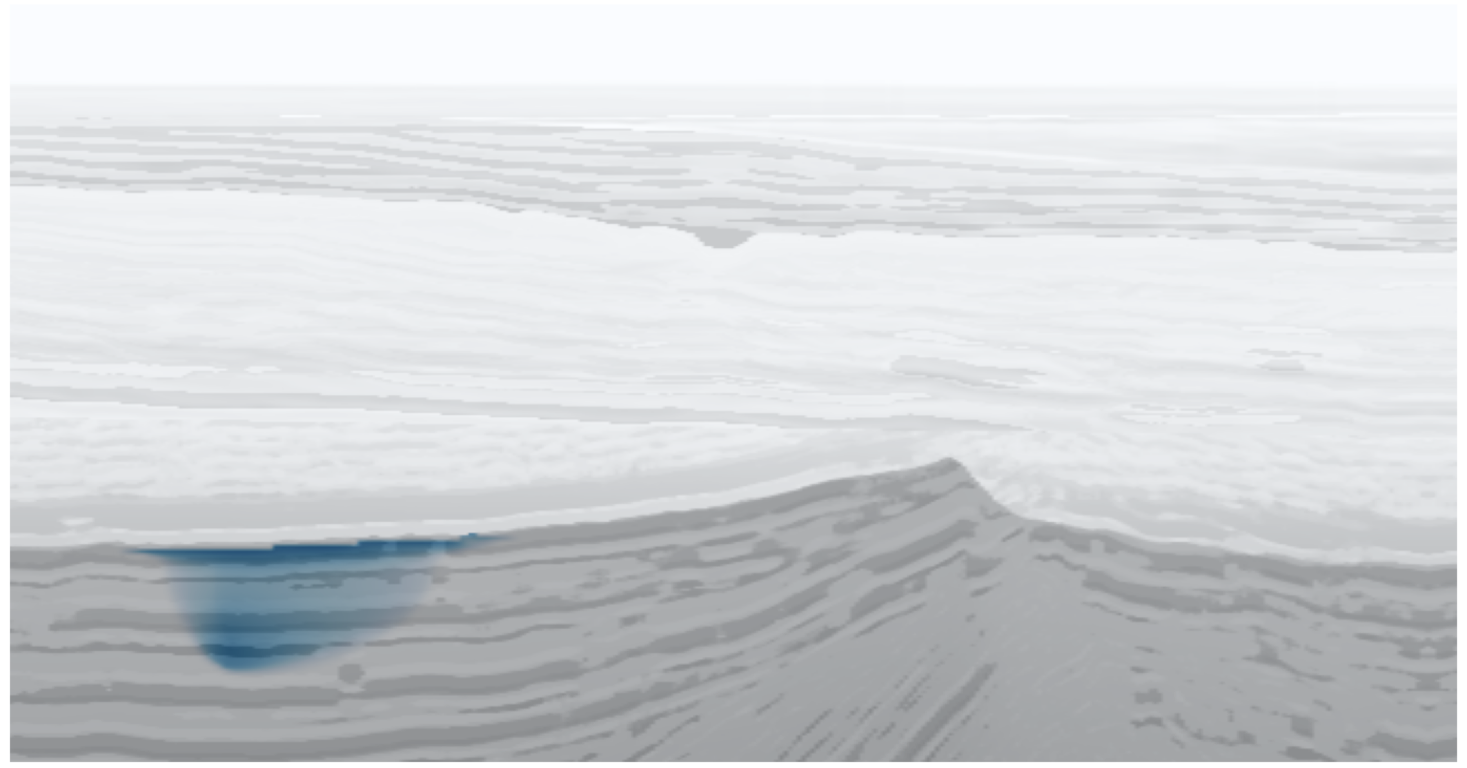

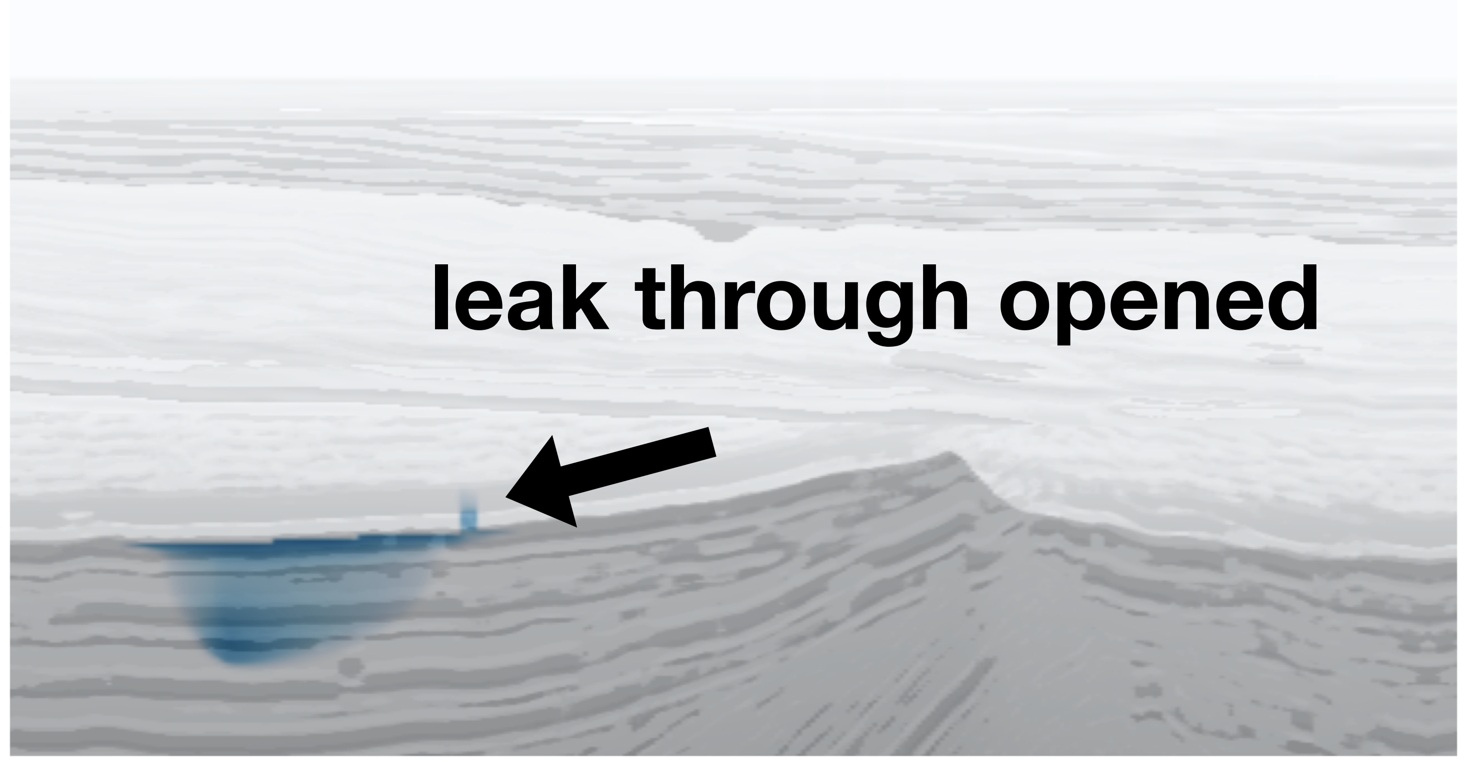

https://github.com/slimgroup/Seis4CCS.jl/blob/main/notebooks/01_FlowSimulation.ipynb

Rock-physics modeling

Workflow


proxy model
wavespeed, density
reservoir model
permeability, porosity
pressure induced fault
two-phase flow
CO_2 dynamics
concentration, pressure
leakage
regular
time-lapse models
wavespeed, density
time-lapse (diff) data
time-lapse imaging
deep neural classifier
leakage
regular
class activation mapping
Confusion Matrix
No Leakage
Leakage
True Neg
193
48.98%
False Pos
13
3.30%
False Neg
41
10.41%
True Pos
147
37.31%
No Leakage
Leakage
accuracy = 86.29%

Rock physics
patchy saturation model

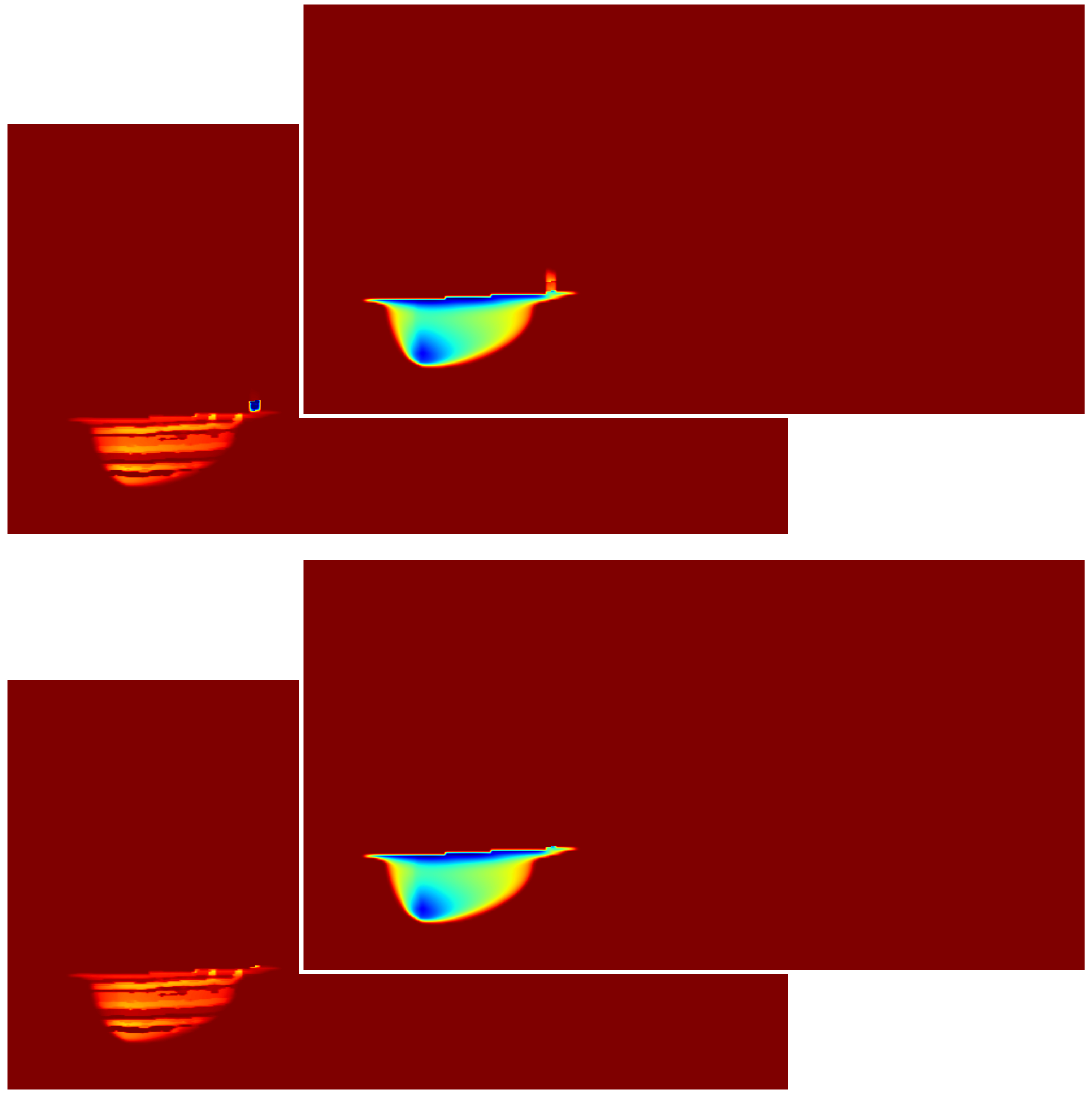

CO₂ concentration ↑ → v_p & ρ ↓

v_p decrease by 0-300 m/s

localized time-lapse changes

1.68% change in acoustic impedance

Symbol	Meaning
B_{r1}/B_{r2}	bulk modulus of rock fully saturated with fluid 1/2
B_{f1}/B_{f2}	fluid bulk modulus
ρ_{f1}/ρ_{f2}	fluid density
μ_r	rock shear modulus
v_p/v_s	rock P/S-wave velocity
B_o	bulk modulus of rock grains
ρ_r	rock density
ϕ	rock porosity
S	CO_2 saturation

$$
\begin{aligned}
B_{r1} &= \rho_r(v_p^2 - \tfrac{4}{3}v_s^2)\\
\mu_r &= \rho_r v_s^2\\
\frac{B_{r2}}{B_o - B_{r2}} &= \frac{B_{r1}}{B_o - B_{r1}} - \frac{B_{f1}}{\phi(B_o - B_{f1})} + \frac{B_{f2}}{\phi(B_o - B_{f2})}\\
\hat{B}_r &= [(1-S)(B_{r1} + \tfrac{4}{3}\mu_r)^{-1} + S(B_{r2} + \tfrac{4}{3}\mu_r)^{-1}]^{-1} - \tfrac{4}{3}\mu_r\\
\hat{\rho}_r &= \rho_r + \phi S(\rho_{f2} - \rho_{f1})\\
\hat{v}_p &= \sqrt{\frac{\hat{B}_r + \frac{4}{3}\mu_r}{\hat{\rho}_r}}
\end{aligned}
$$

Per Avseth, et al. Quantitative seismic interpretation: Applying rock physics tools to reduce interpretation risk. Cambridge university press, 2010.
https://github.com/slimgroup/Seis4CCS.jl/blob/main/src/RockPhysics/RockPhysicsFunctions.jl

Seismic modeling

Workflow

proxy model
wavespeed, density
reservoir model
permeability, porosity
pressure
induced
fault
two-phase
flow
CO_2 dynamics
concentration, pressure
leakage
regular
time-lapse models
wavespeed, density
time-lapse (diff) data
time-lapse imaging
deep neural classifier
leakage
regular
class activation mapping
Confusion Matrix
No Leakage
Leakage
True Neg
193
48.98%
False Pos
13
3.30%
False Neg
41
10.41%
True Pos
147
37.31%
No Leakage
Leakage
accuracy = 86.29%

Setup

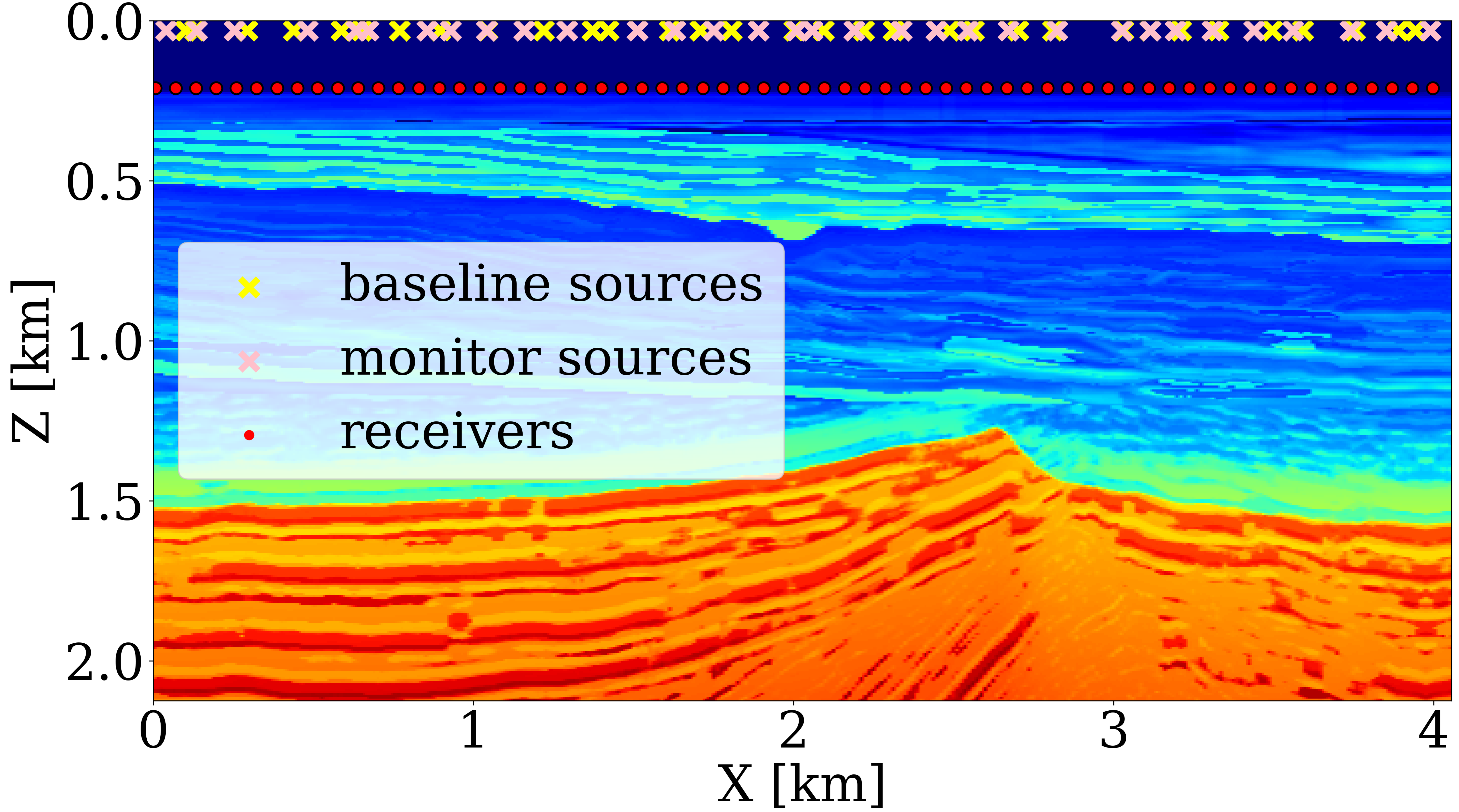

- 32 non-replicated source locations (average source sampling 125m)
- 162 hydrophones 2m above ocean bottom (average receiver sampling 25m)
- Ricker wavelet w/ central frequency 25 Hz

Seismic time-lapse

simulations

```
# Generate nv vintages of linear data
F0 = [Pr*judiModeling(model0)*Ps[i]' for I=1:nv]          # forward modeling
J  = [judiJacobian(F0[i], q[i]) for i=1:nv]               # linearized born modeling
dlin = J .* dimp                                          # generate linear data
# add band-limited noise
noise = deepcopy(dlin)
for k = 1:nv
    for l = 1:nsrc
        # filter white noise by source wavelet
        noise[k].data[l] = real.(ifft(fft(randn(Float32, size(dlin[k].data[l]))).*fft(q[k].data[1])))
    end
end
snr   = 8.0f0
noise = noise/norm(noise) * norm(dlin) * 10f0^(-snr/20f0)
dlin  = dlin + noise                                      # 8 dB additive noise
```

- linearized Born modeling (demigration)
- SNR 8 dB by adding white noise filtered w/ source wavelet

https://github.com/slimgroup/GCS-CAM/blob/main/scripts/GenLinData.jl

Time-lapse imaging

Workflow


proxy model
wavespeed, density
reservoir model
permeability, porosity
pressure induced fault
two-phase flow
CO_2 dynamics
concentration, pressure
leakage
regular
time-lapse models
wavespeed, density
class activation mapping
deep neural classifier
time-lapse imaging
time-lapse (diff) data
Confusion Matrix
True Neg
193
48.98%
False Pos
13
3.30%
False Neg
41
10.41%
True Pos
147
37.31%
No Leakage
Leakage
No Leakage
Leakage
accuracy = 86.29%
leakage
regular

Joint imaging

joint recovery model

Invert $\mathbf{A}\mathbf{z} = \mathbf{b}$ where

$$\mathbf{A} = \begin{bmatrix} \frac{1}{\gamma}\mathbf{A}_1 & \mathbf{A}_1 & & & \\ \frac{1}{\gamma}\mathbf{A}_2 & & \mathbf{A}_2 & & \\ \cdots & & & \cdots & \\ \frac{1}{\gamma}\mathbf{A}_{n_v} & & & & \mathbf{A}_{n_v} \end{bmatrix} \qquad \mathbf{z} = \left[\mathbf{z}_0^\top, \mathbf{z}_1^\top, \cdots, \mathbf{z}_{n_v}^\top\right]^\top$$

common component innovation components

γ $(0 < \gamma < n_v)$ controls weight on *common* component

1st column adds complementary info when $\mathbf{A}_i \neq \mathbf{A}_j$

exploit shared information

No need to *replicate* to get high degrees of repeatability

https://github.com/slimgroup/GCS-CAM/blob/main/scripts/JRM.jl

Witte, P. A., Louboutin, M., Luporini, F., Gorman, G. J., & Herrmann, F. J. (2019). Compressive least-squares migration with on-the-fly Fourier transforms. *Geophysics*, *84*(5), R655-R672.
Yang, M., Fang, Z., Witte, P., & Herrmann, F. J. (2020). Time-domain sparsity promoting least-squares reverse time migration with source estimation. *Geophysical Prospecting*, *68*(9), 2697-2711.

Optimization

linearized Bregman Iterations

Solve via curvelet-domain sparsity promotion:

$$\min_{\mathbf{x}} \quad \lambda \|\mathbf{C}\mathbf{x}\|_1 + \frac{1}{2}\|\mathbf{C}\mathbf{x}\|_2^2$$
$$\text{subject to} \quad \|\mathbf{b} - \mathbf{A}\mathbf{x}\|_2^2 \leq \sigma^2$$

for $k = 1,2,\ldots$

$$\mathbf{u}^{k+1} = \mathbf{u}^k - t^k \mathbf{A}^{(k)^\top}(\mathbf{A}^{(k)}\mathbf{x}^k - \mathbf{b}^{(k)})$$
$$\mathbf{x}^{k+1} = \mathbf{C}^\top S(\mathbf{C}\mathbf{u}^{k+1}, \lambda)$$

C – curvelet transform

$\mathbf{A}^{(k)}, \mathbf{b}^{(k)}$ – the demigration operator for randomly (w/ replacement) selected shots

$S(t,\lambda) = \max\{|t| - \lambda, 0\}$sign$(t)$ – soft thresholding w/ threshold λ

Ziyi Yin, Huseyin Tuna Erdinc, Abhinav Prakash Gahlot, Mathias Louboutin and F. Herrmann. “Derisking geological carbon storage from high-resolution time-lapse seismic to explainable leakage detection.” The Leading Edge (2023).
Ziyi Yin, Mathias Louboutin, and Felix J. Herrmann. "Compressive time-lapse seismic monitoring of carbon storage and sequestration with the joint recovery model." *IMAGE*. 2021.

Seismic imaging

JRM vs RTM

JRM

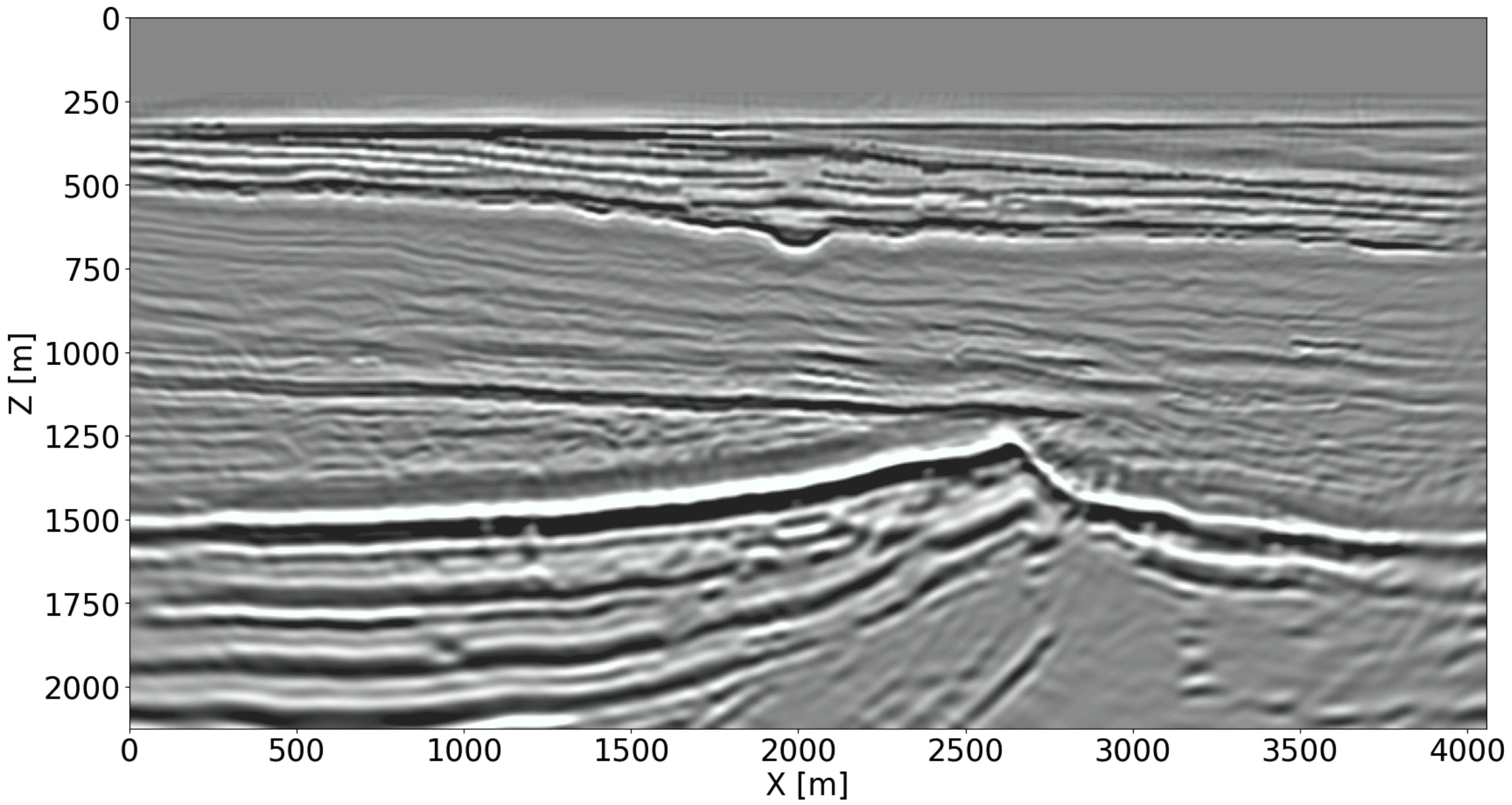

RTM

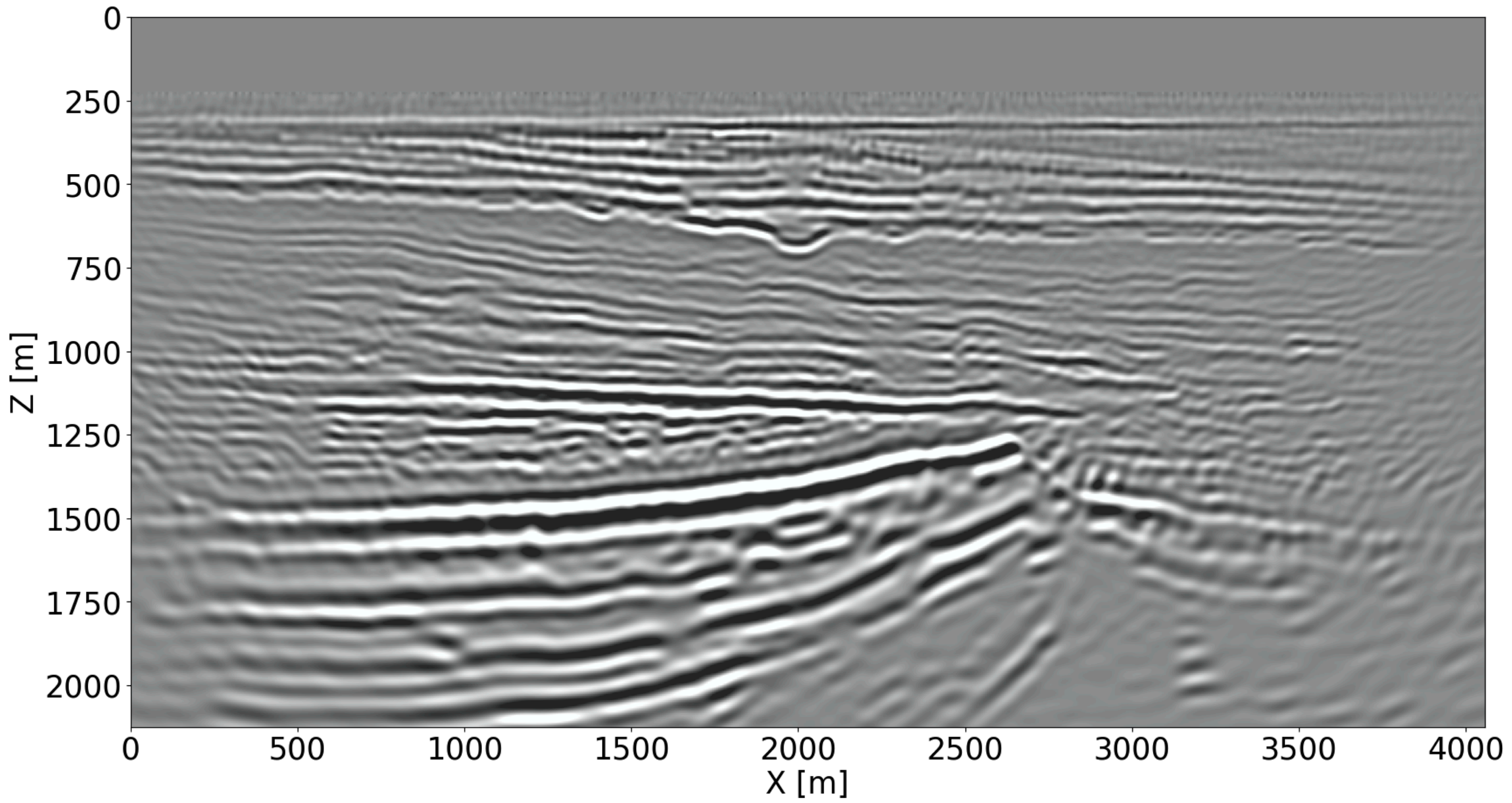

Number of iterations: 22

Batch size: 4

Number of sources: 32

Number of data passes: 3

Ziyi Yin, Huseyin Tuna Erdinc, Abhinav Prakash Gahlot, Mathias Louboutin and F. Herrmann. “De-risking geological carbon storage from high resolution time-lapse seismic to explainable leakage detection.” The Leading Edge (2023).
Ziyi Yin, Mathias Louboutin, and Felix J. Herrmann. "Compressive time-lapse seismic monitoring of carbon storage and sequestration with the joint recovery model." *IMAGE*. 2021.

Time-lapse differences

$$\textbf{NRMS} = 200\% \times \frac{\|\mathbf{x}_1 - \mathbf{x}_2\|}{\|\mathbf{x}_1\| + \|\mathbf{x}_2\|}$$

Independent RTMs
NRMS = 8.48%

JRM
NRMS = 3.20%

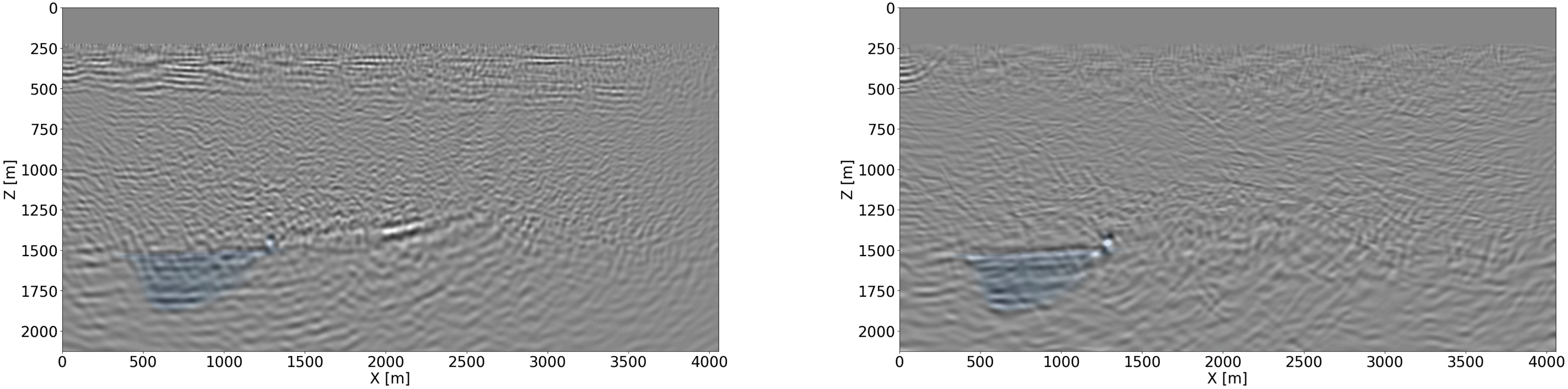

SLIM
ML4Seismic

Automatic leakage detection w/ explainable ML

Ziyi Yin, Huseyin Tuna Erdinc, Abhinav Prakash Gahlot, Mathias Louboutin and F. Herrmann. “Derisking geological carbon storage from high-resolution time-lapse seismic to explainable leakage detection.” The Leading Edge (2023).
Erdinc, H. T., Gahlot, A. P., Yin, Z., Louboutin, M., & Herrmann, F. J. De-risking Carbon Capture and Sequestration with Explainable CO2 Leakage Detection in Time-lapse Seismic Monitoring Images. *AAAI Symposium (2022)*

Jones, C., Edgar, J., Selvage, J., and Crook, H., 2012, Building complex synthetic models to evaluate acquisition geometries and velocity inversion technologies: In 74th EAGE conference and exhibition, pp. cp–293

Training set

Compass model

Five different 2D velocity slices

1000 leak/no leak scenarios

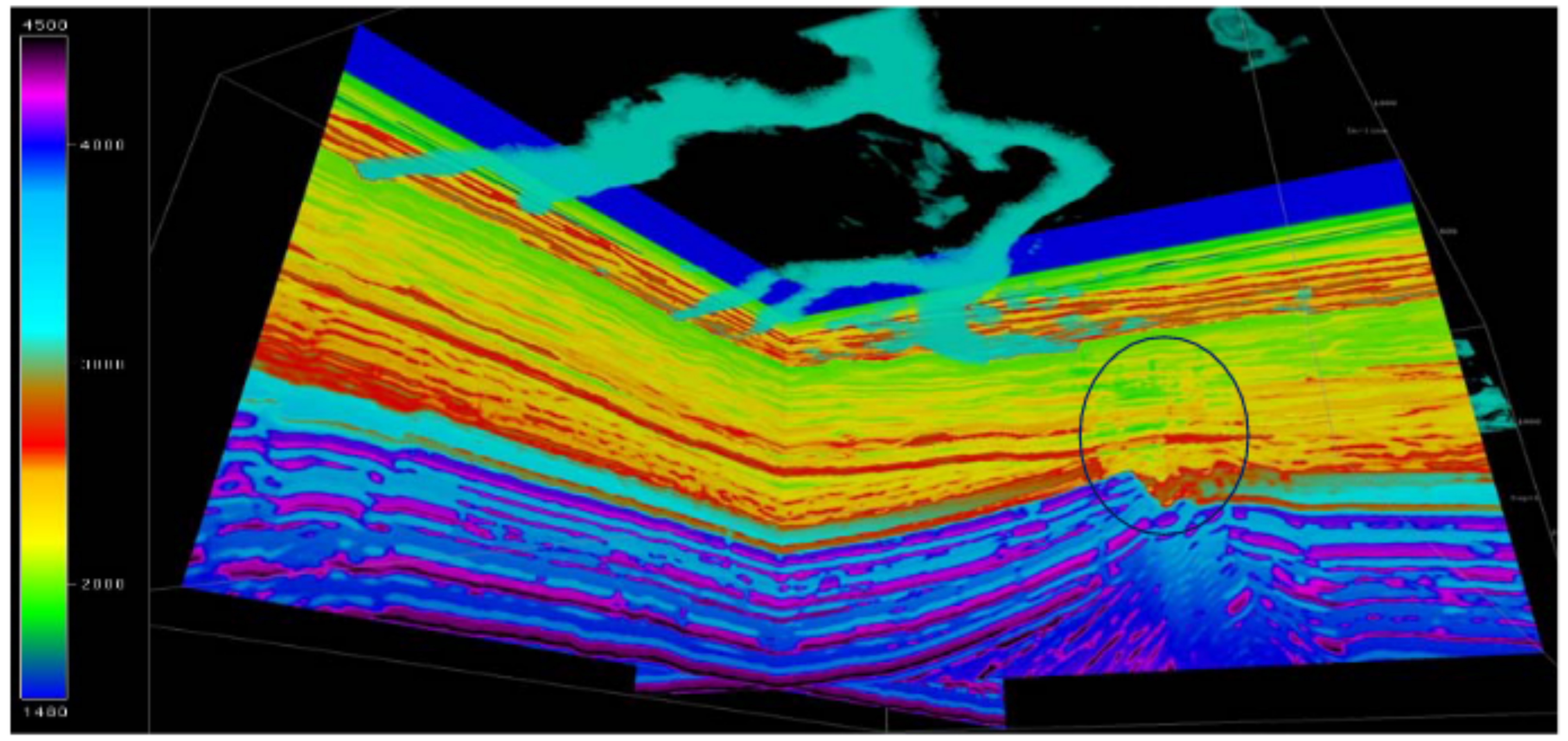

Retrieved from Jones (2008)

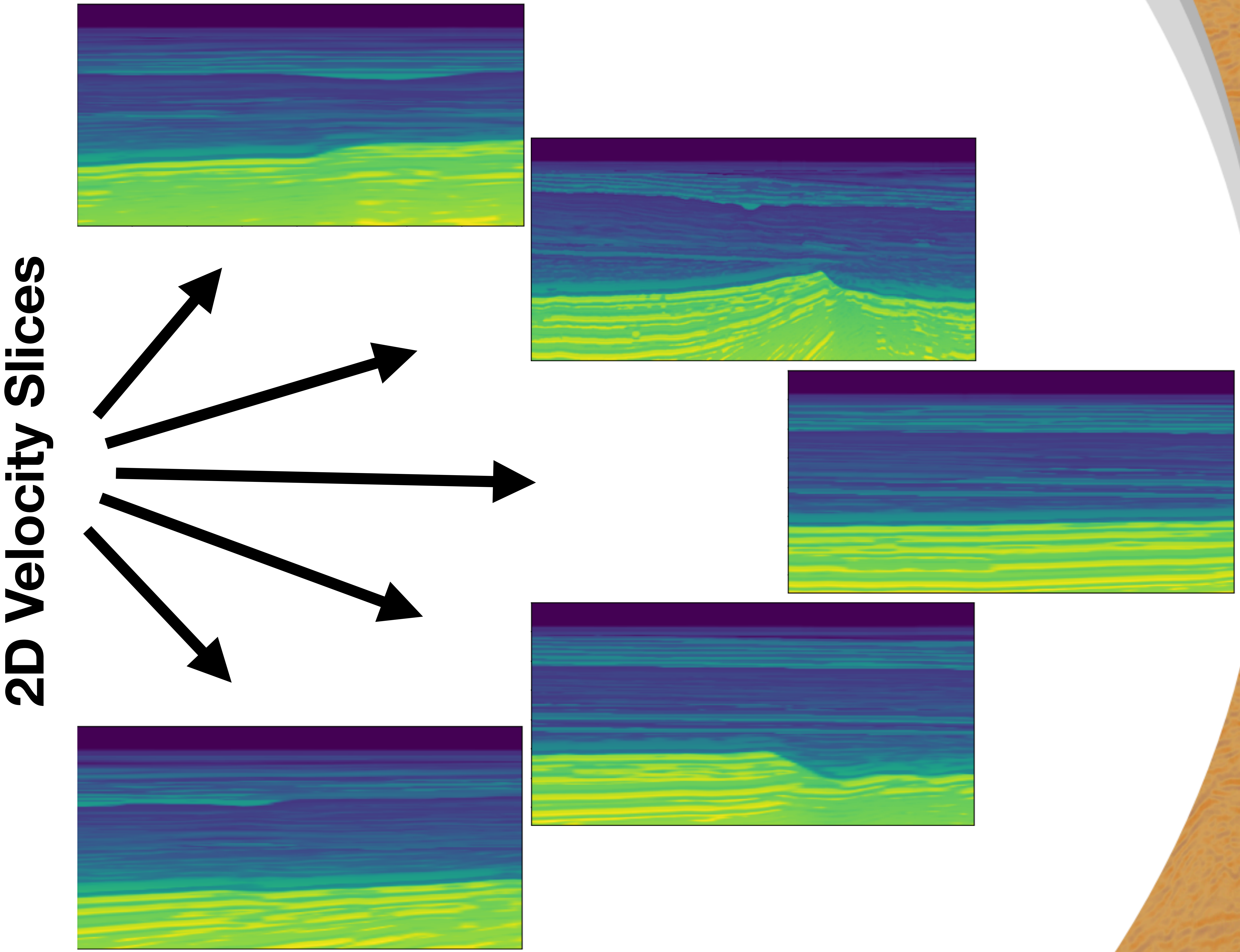

Ziyi Yin, Huseyin Tuna Erdinc, Abhinav Prakash Gahlot, Mathias Louboutin, and Felix J. Herrmann, "**Derisking geological carbon storage from high-resolution time-lapse seismic to explainable leakage detection**", The Leading Edge, vol. 42, pp. 69–76, 2023.

SLIM ML4Seismic

Training dataset

densely sampled seismic data

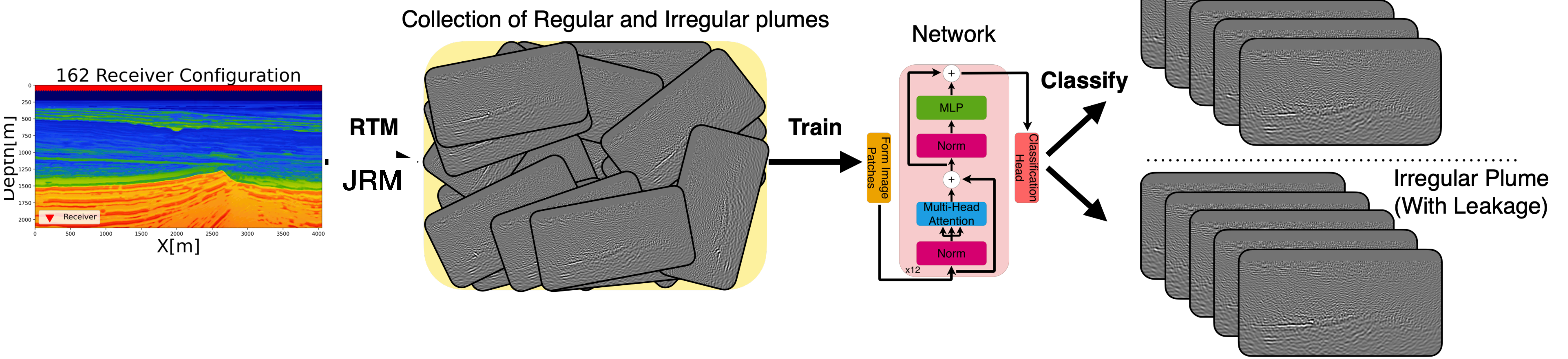

- pressure ≥ 15MPa seal opens $(12.5\,\mathrm{m} - 62.5\,\mathrm{m})$ randomly
- permeability $10^{-4}\,\mathrm{md} \rightarrow 500\,\mathrm{md}$
- linear time-lapse data generated w/ & w/o leakage
- time-lapse data inverted after 200 days w/ JRM

https://github.com/slimgroup/GCS-CAM/blob/main/scripts/JRM.jl

Seismic imaging
no leakage

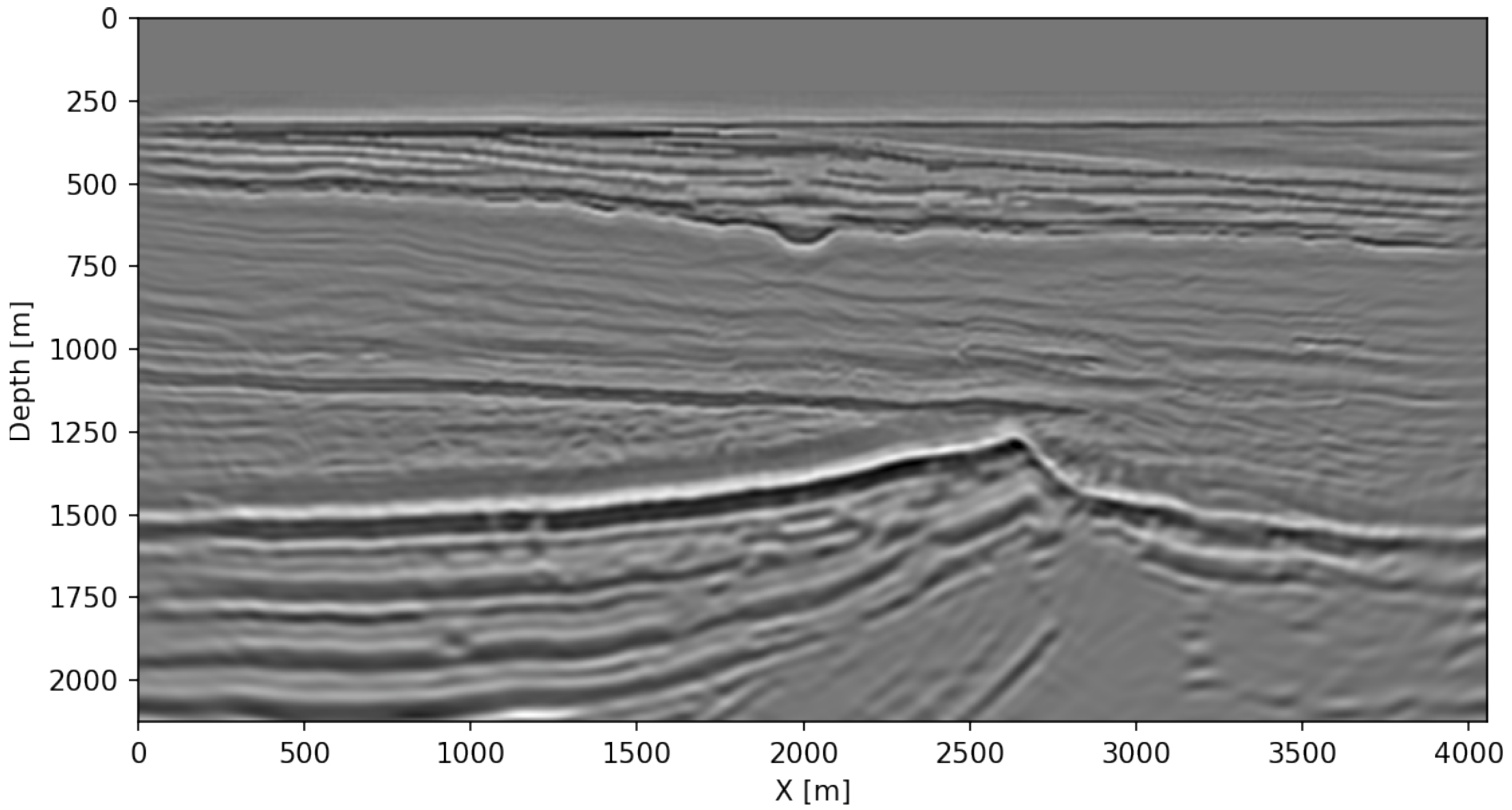

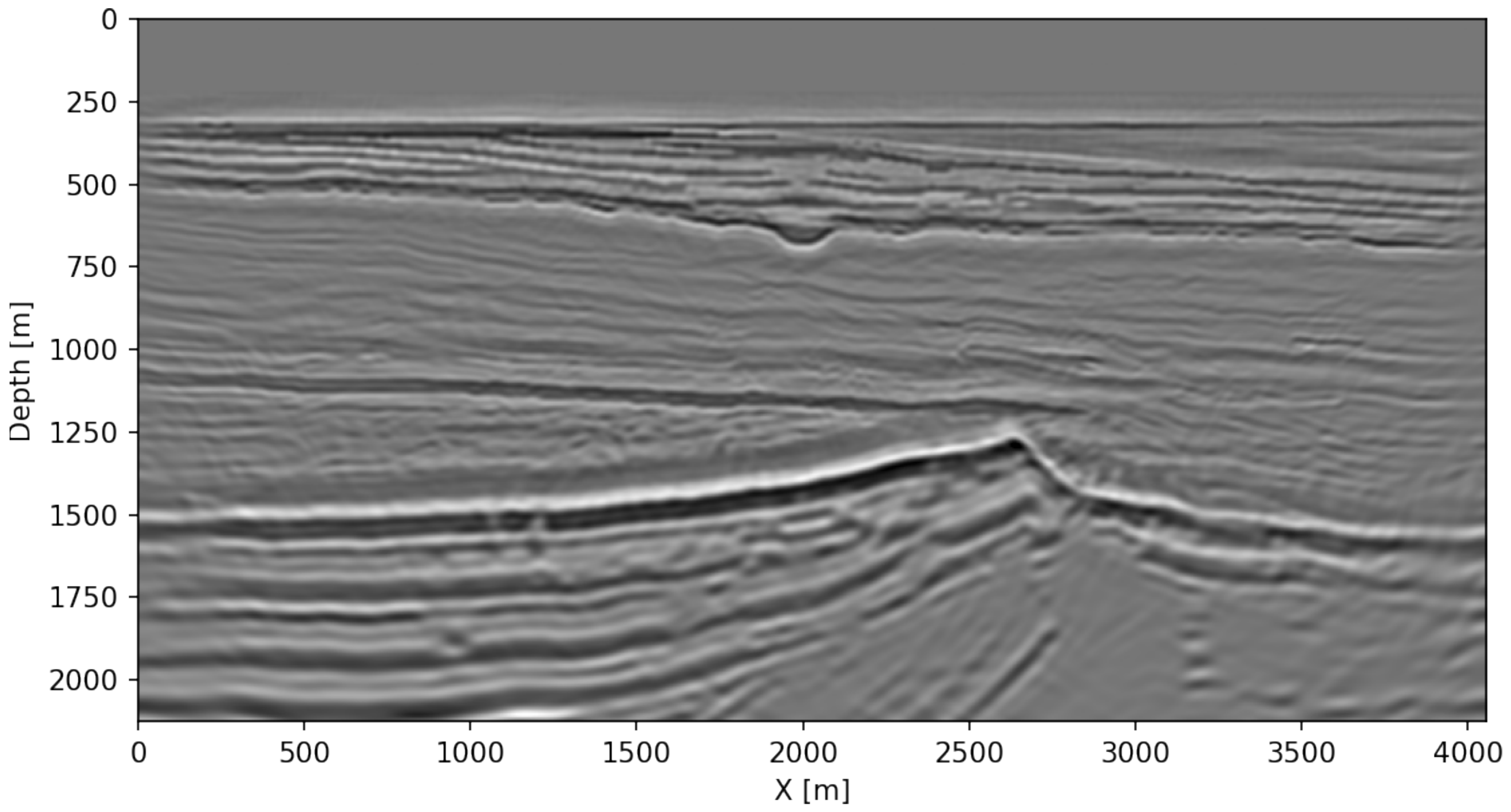

10X no leakage difference image

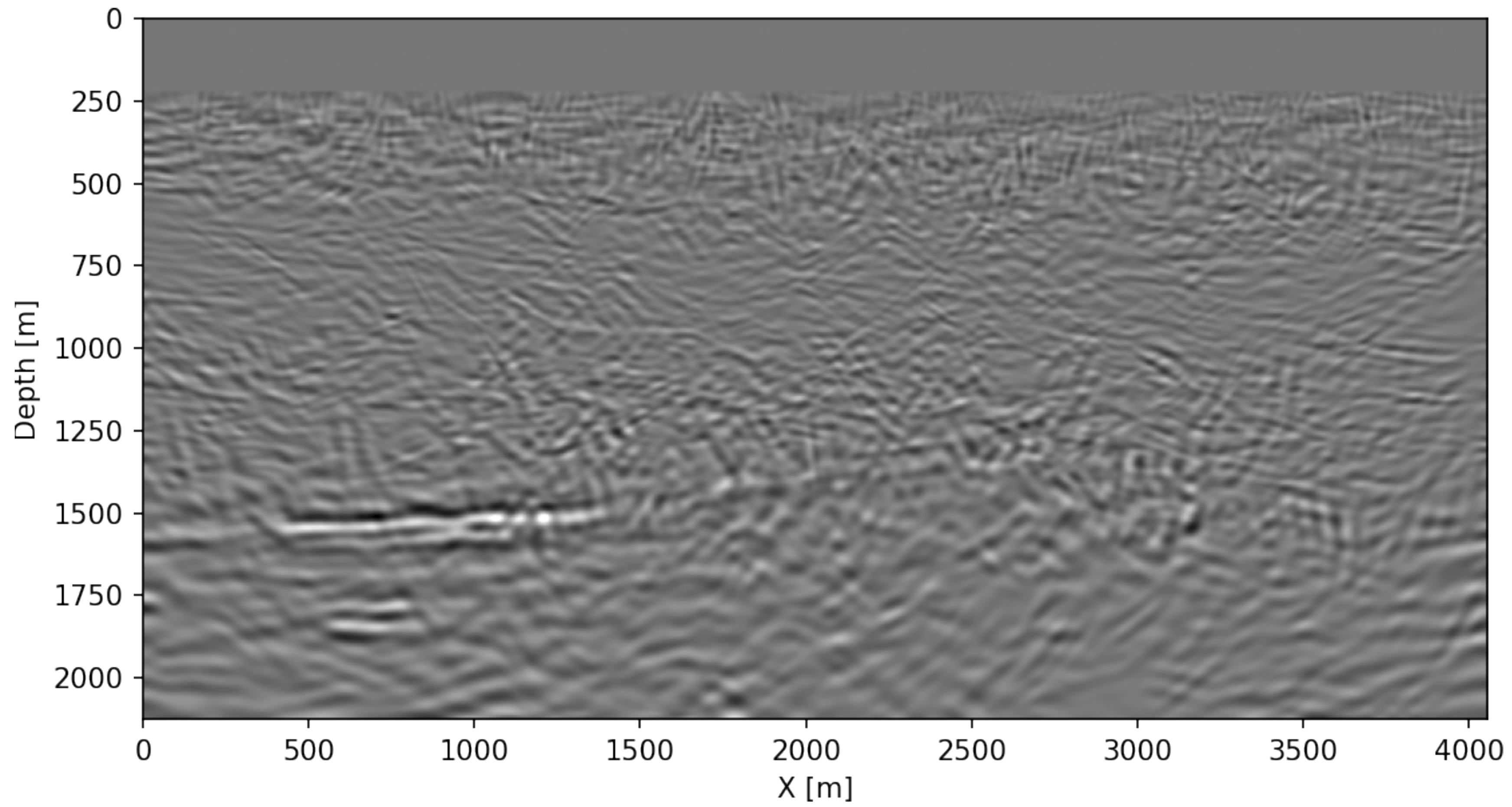

Difference images will be network input

SLIM
ML4Seismic

Seismic imaging
leakage

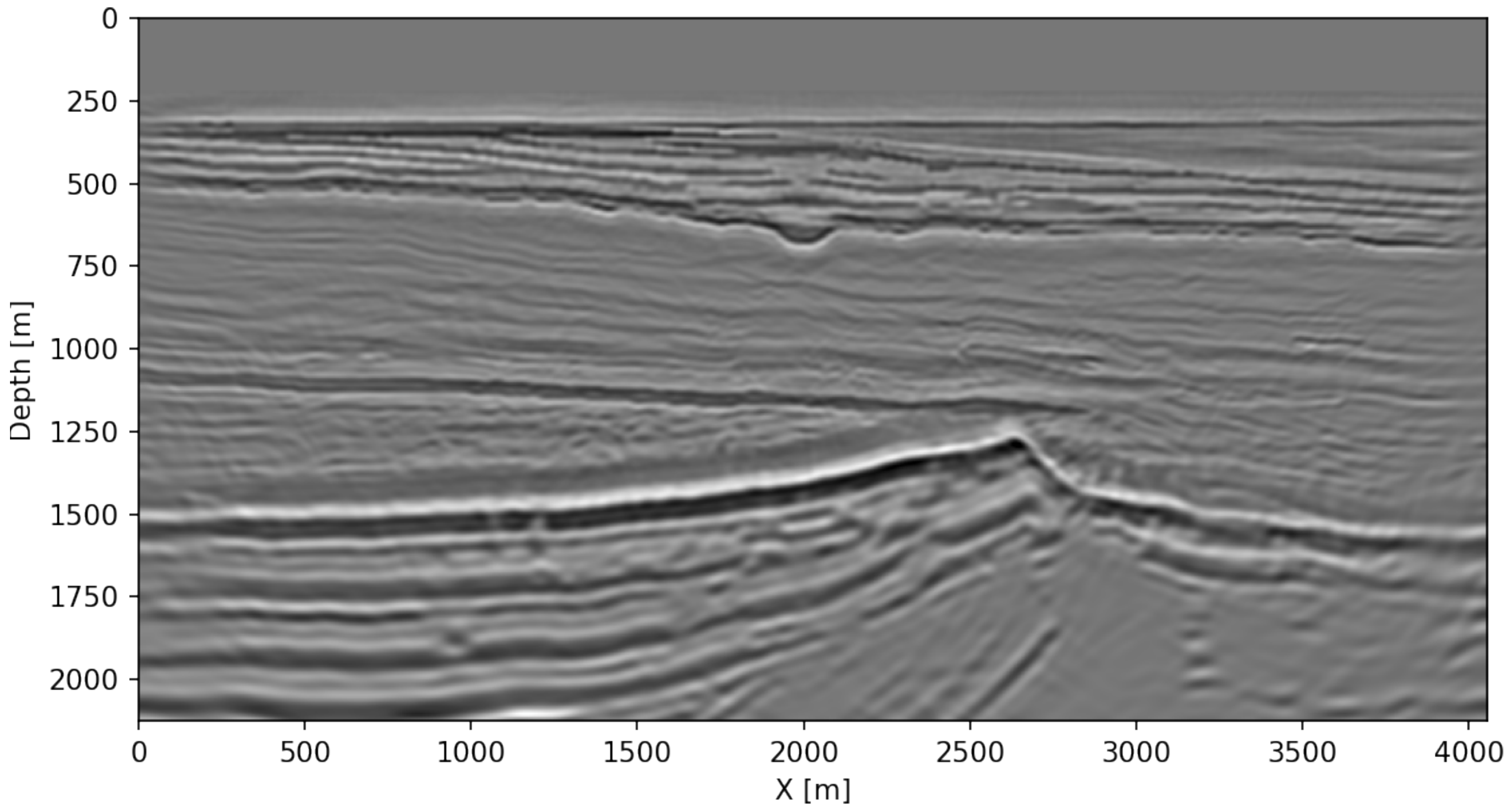

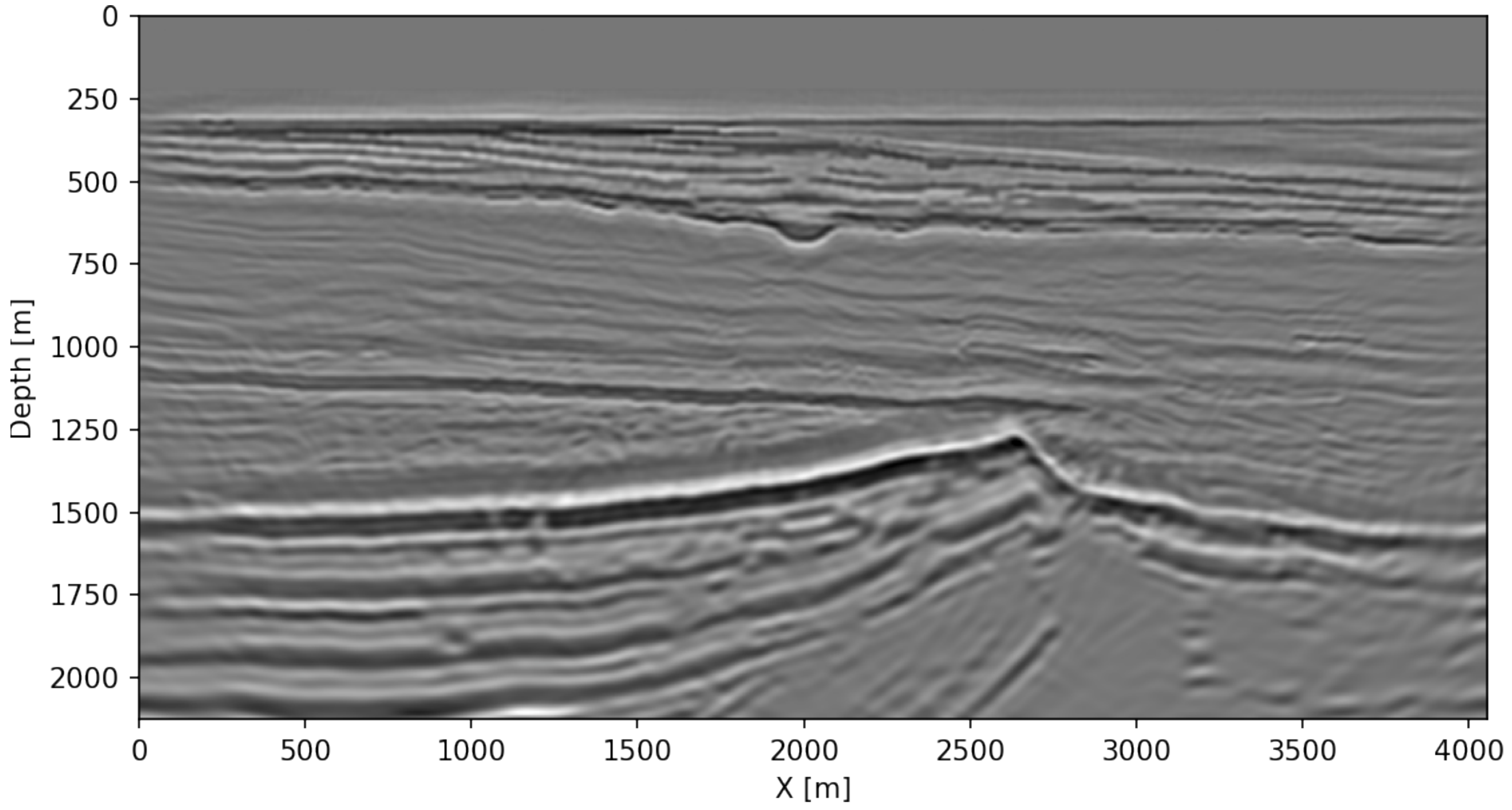

10X leakage difference image

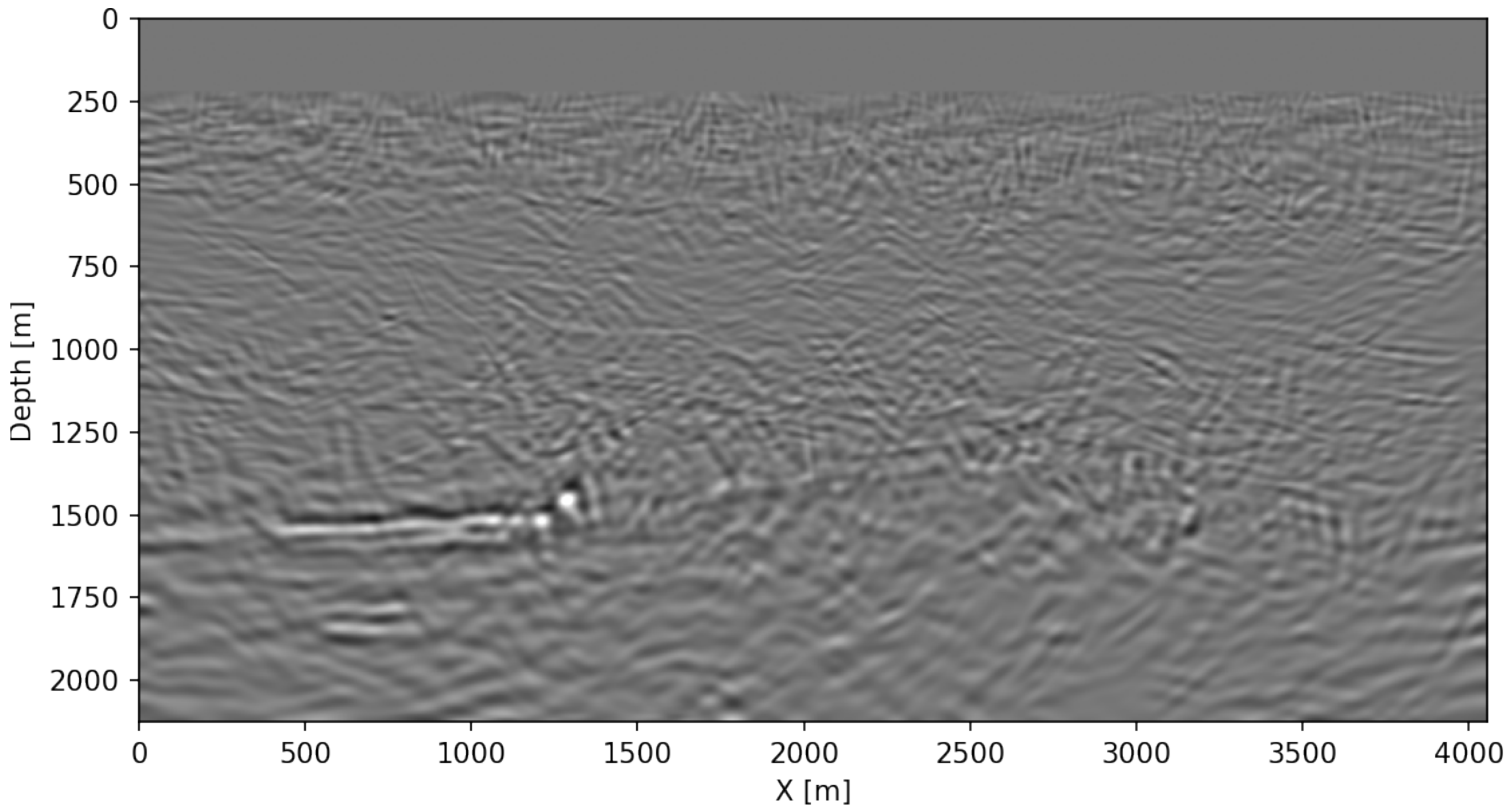

Difference images will be network input

JRM vs independent Imaging

NRMS histogram

JRM:

- lower NRMS
- narrower range
- **6~7% → 2~3%**
- more *repeatable* recovery

NRMS statistics

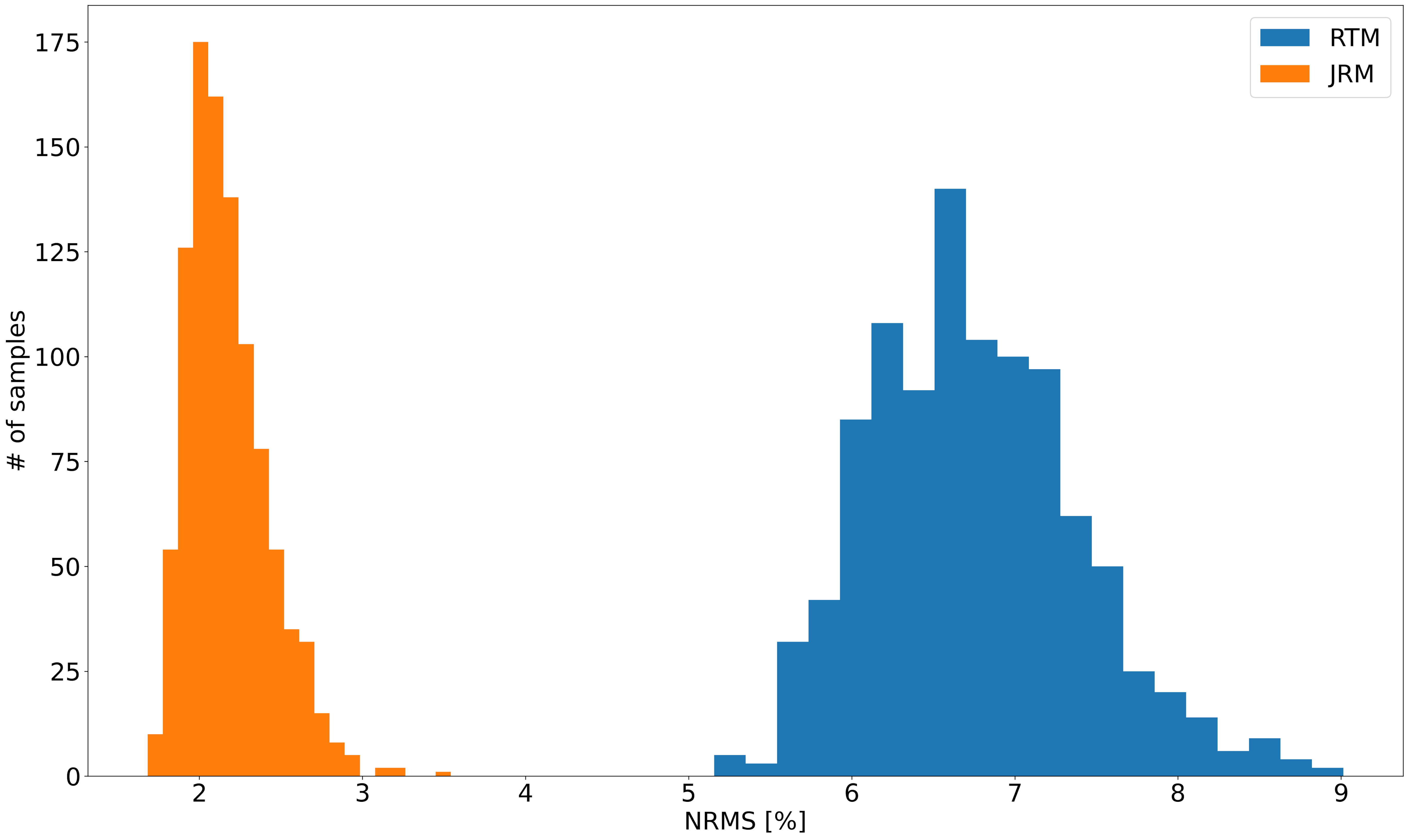

SLIM
ML4Seismic

Class activation mapping

Workflow


proxy model
wavespeed, density
reservoir model
permeability, porosity
pressure
induced
fault
two-phase
flow
CO_2 dynamics
concentration, pressure
leakage
regular
time-lapse models
wavespeed, density
time-lapse (diff) data
time-lapse imaging
deep neural classifier
leakage
regular
class activation mapping
Confusion Matrix
True Neg
193
48.98%
False Pos
13
3.30%
False Neg
41
10.41%
True Pos
147
37.31%
No Leakage
Leakage
No Leakage
Leakage
accuracy = 86.29%

Dosovitskiy, A., Beyer, L., Kolesnikov, A., Weissenborn, D., Zhai, X., Unterthiner, T., ... & Houlsby, N. (2020). An image is worth 16x16 words: Transformers for image recognition at scale. *arXiv preprint arXiv:2010.11929*.

Classification

network training

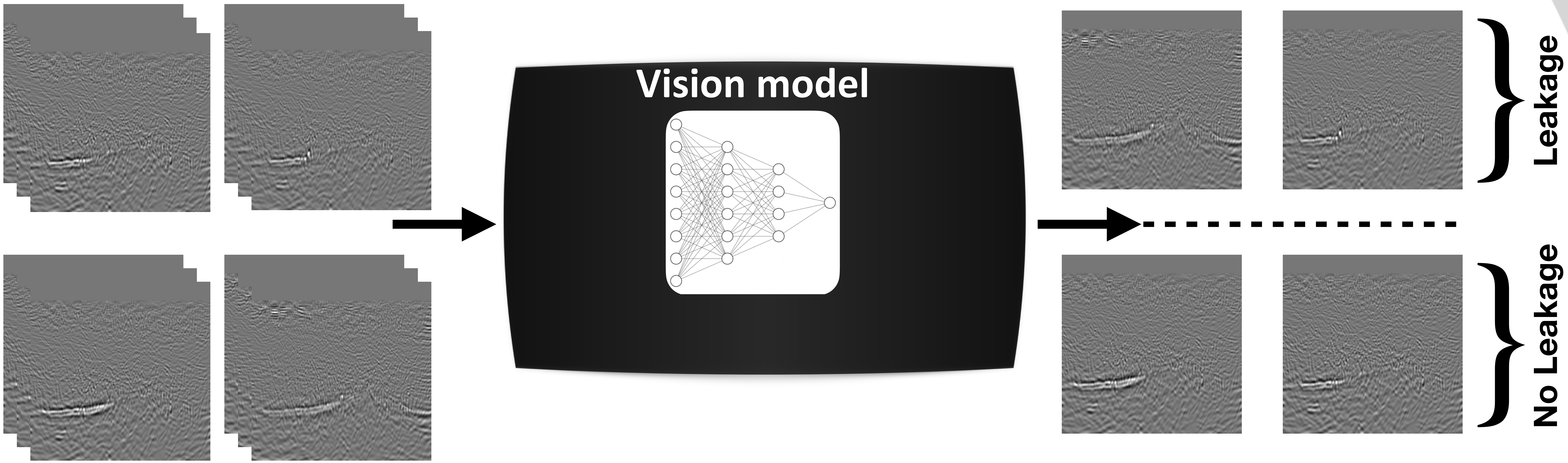

Convert time-lapse difference images to 224x224 size w/ 3 channels

Use state-of-the-art pre-trained vision transformer

https://github.com/slimgroup/GCS-CAM/blob/main/scripts/main.ipynb

Results

Class Activation Mapping

leakage regular

plume

CAM

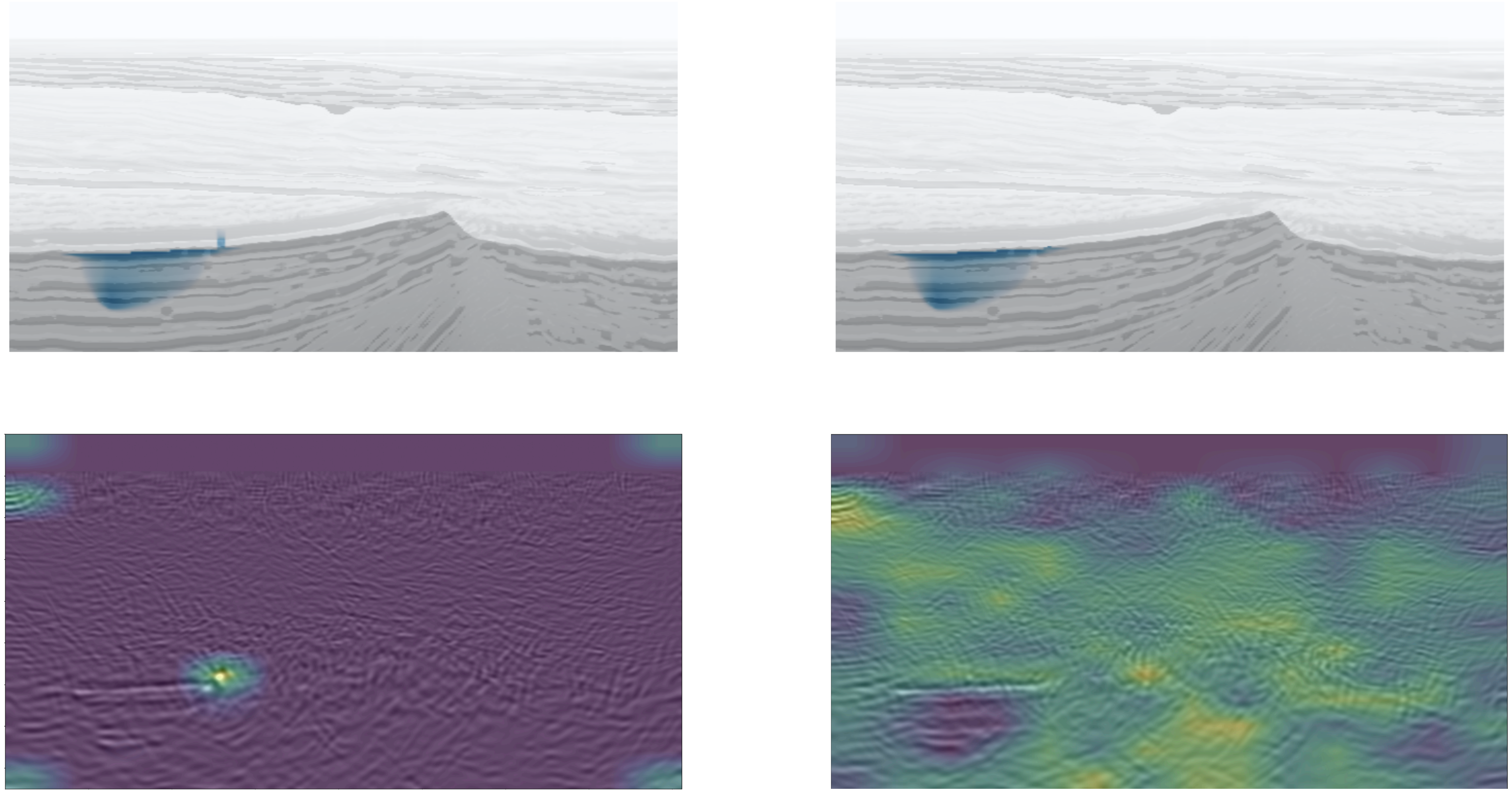

Examples

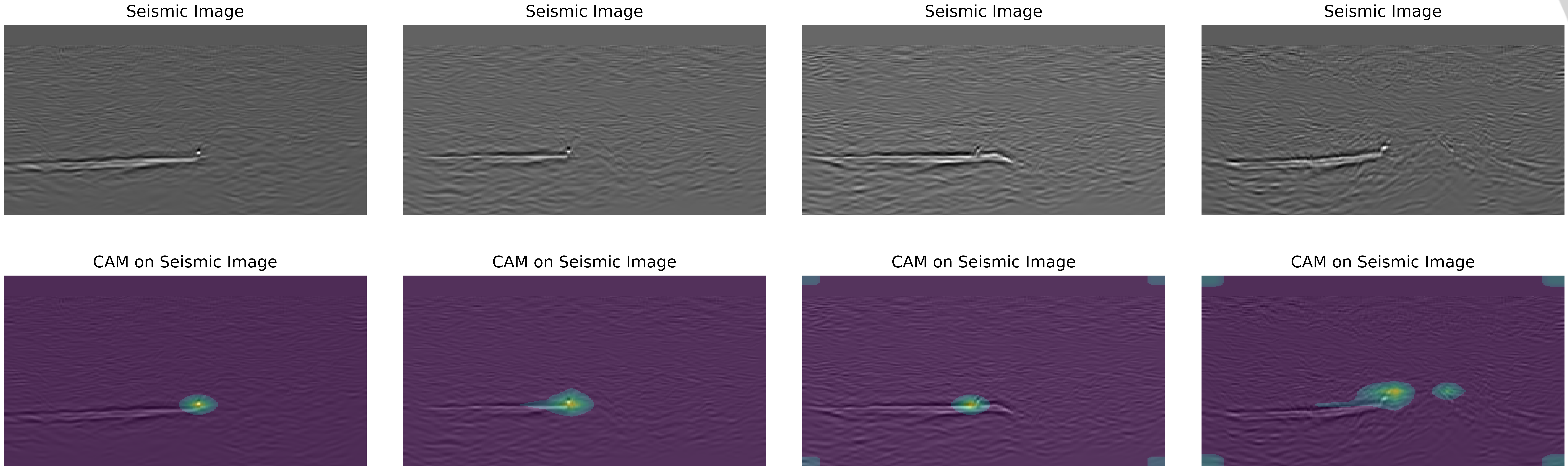

Thresholded CAM maps (<0.2)

Localized areas of (potential) leakage

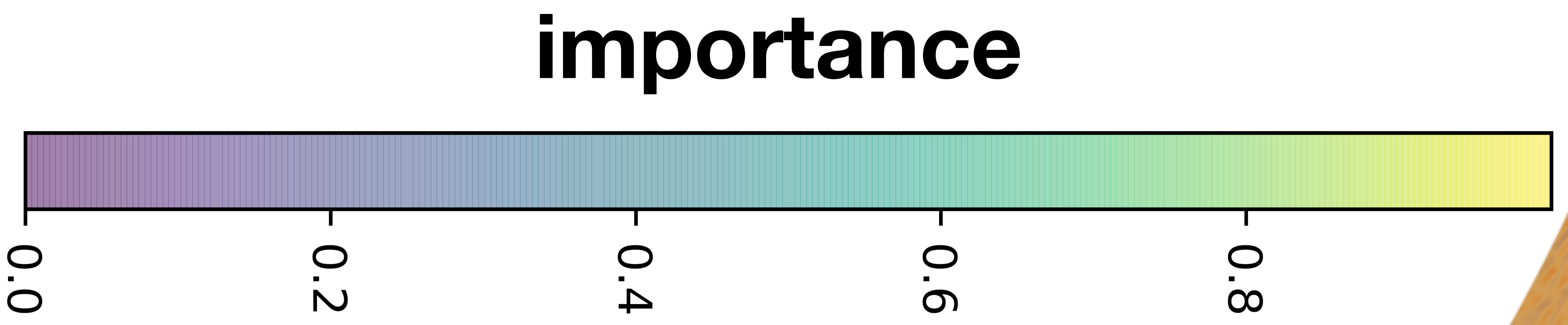

SLIM
ML4Seismic

Results

Overall 86.29% accuracy

- relied on *dense* receiver *sampling*
- relatively *high* percentage *false negatives*
- fewer *false positives*
- may need improvement

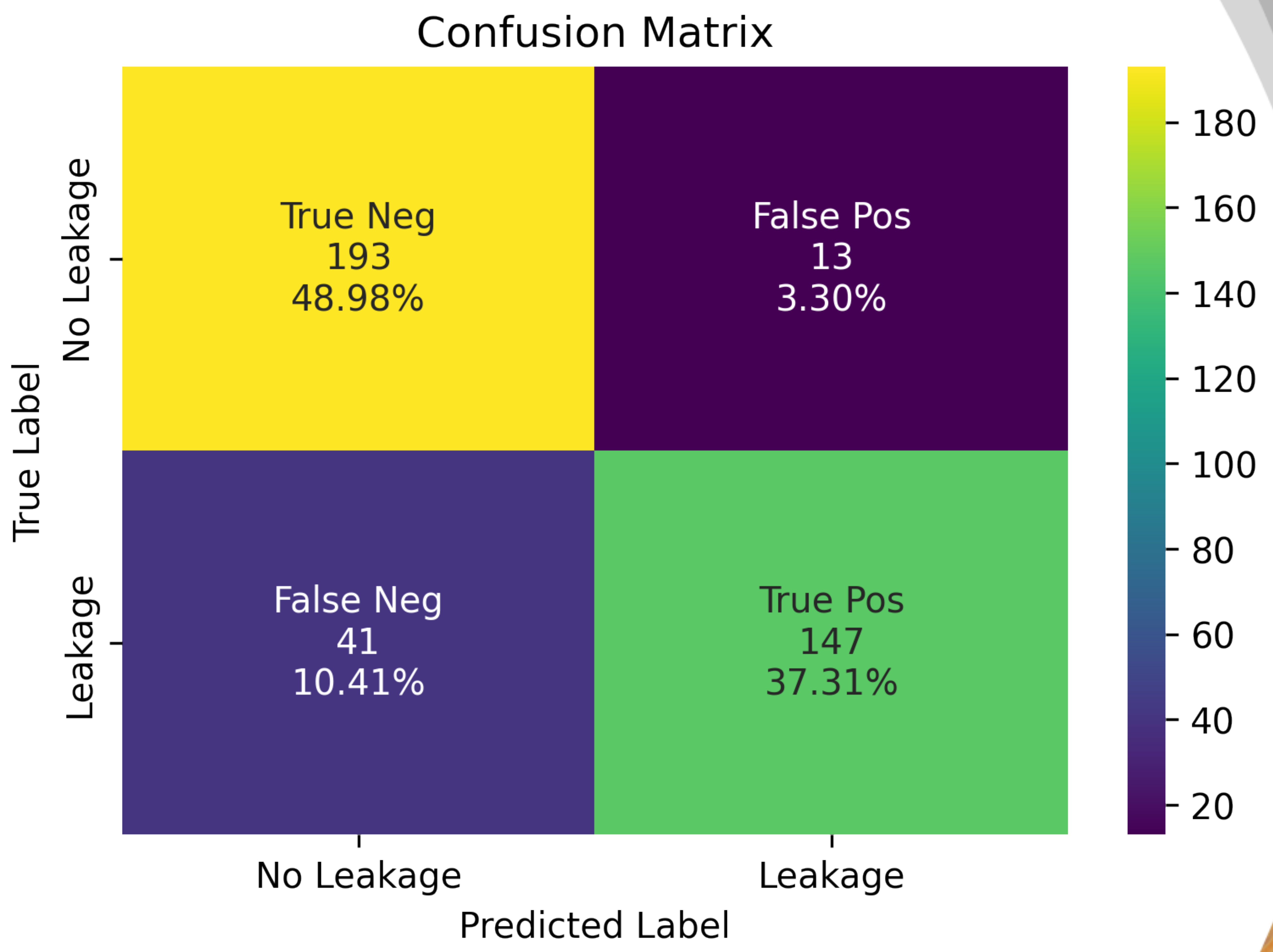

https://github.com/slimgroup/GCS-CAM/blob/main/scripts/main.ipynb

Improved leakage detection w/ data augmentation

Huseyin Tuna Erdinc, Abhinav Prakash Gahlot, Mathias Louboutin, and Felix J. Herrmann, "**Enhancing CO2 Leakage Detectability via Dataset Augmentation**". 2023

SLIM ML4Seismic

Problem

leakage detection deteriorates

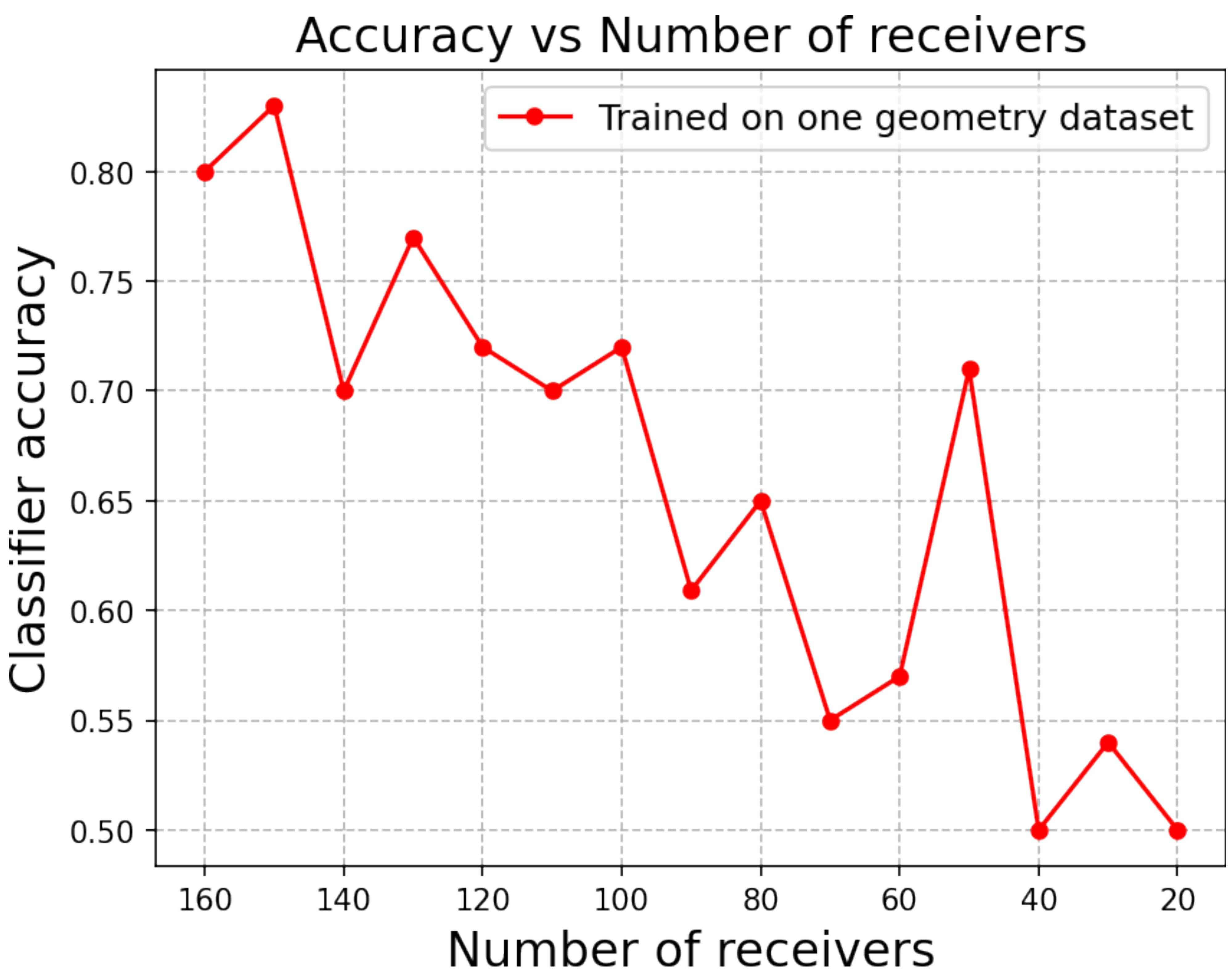

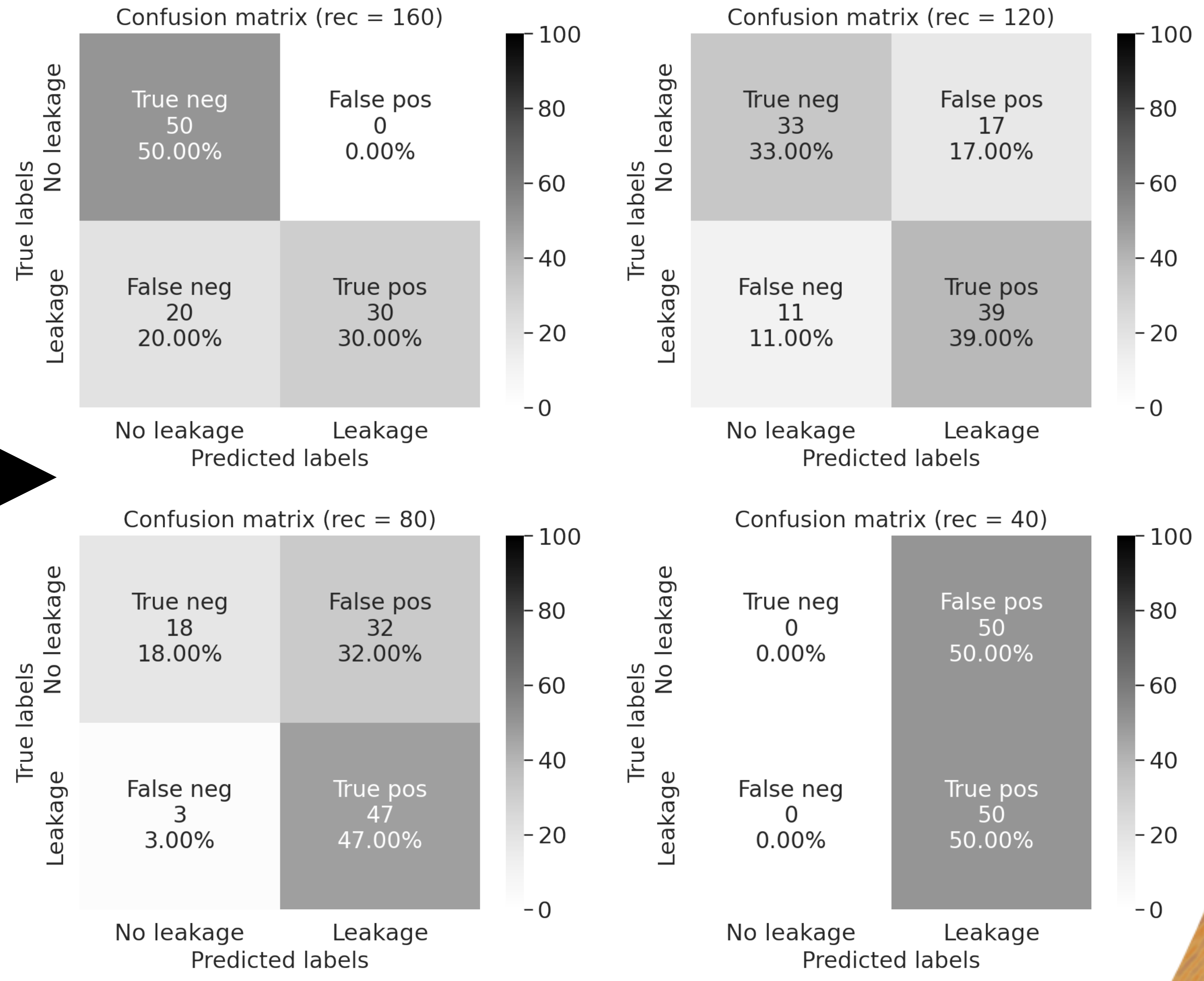

- accuracy *decreases* w/ receiver *density*
- solution *augment* training set

Issue

sparse receiver sampling

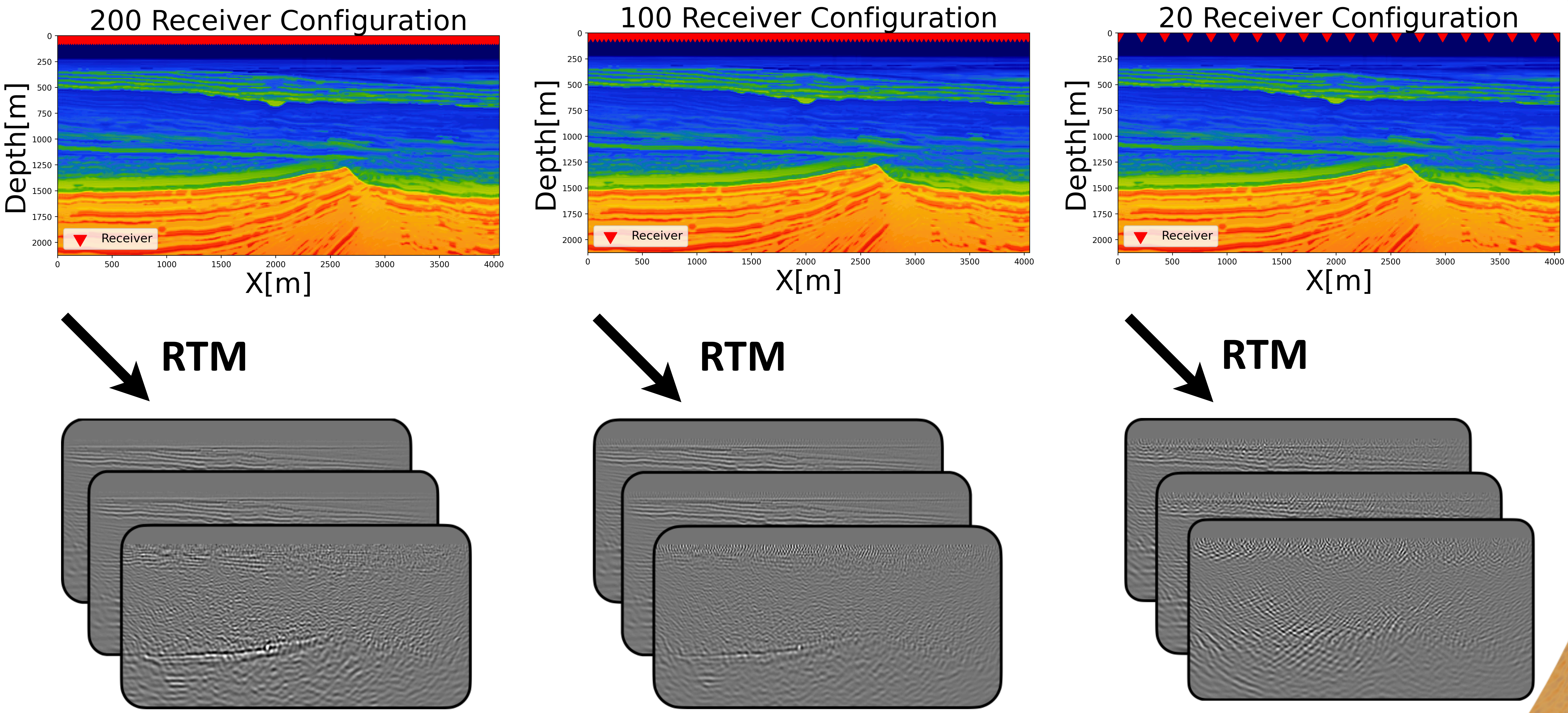

Huseyin Tuna Erdinc, Abhinav Prakash Gahlot, Mathias Louboutin, and Felix J. Herrmann, "Enhancing CO2 Leakage Detectability via Dataset Augmentation". 2023.

SLIM ML4Seismic

Solution

data augmentation

- produce difference images w/ random number of receivers
- add new images to training dataset
- retrain the model w/ augmented dataset
- test on different receiver configurations

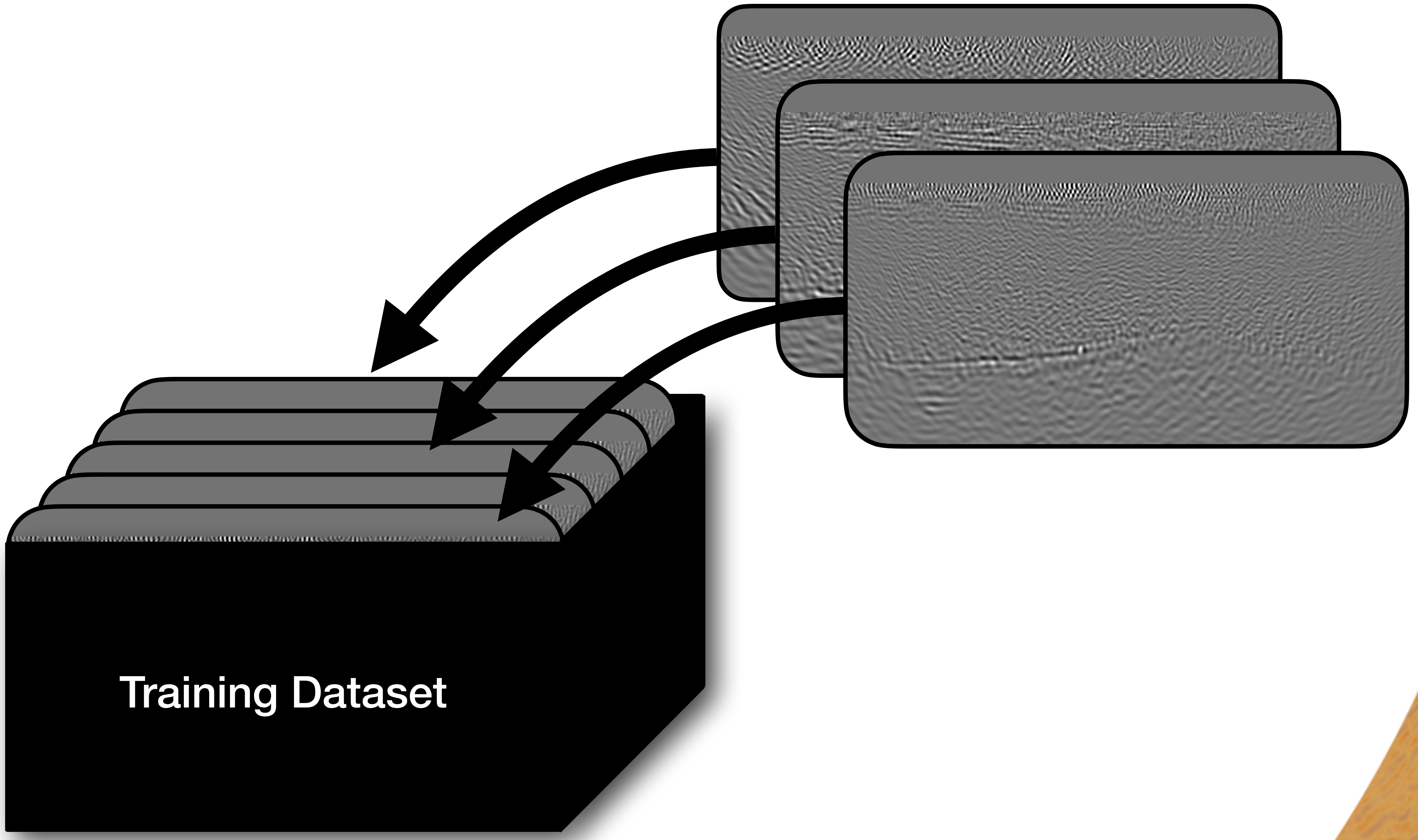

Huseyin Tuna Erdinc, Abhinav Prakash Gahlot, Mathias Louboutin, and Felix J. Herrmann, “**Enhancing CO2 Leakage Detectability via Dataset Augmentation**”. 2023

SLIM ML4Seismic

Results

after data augmentation

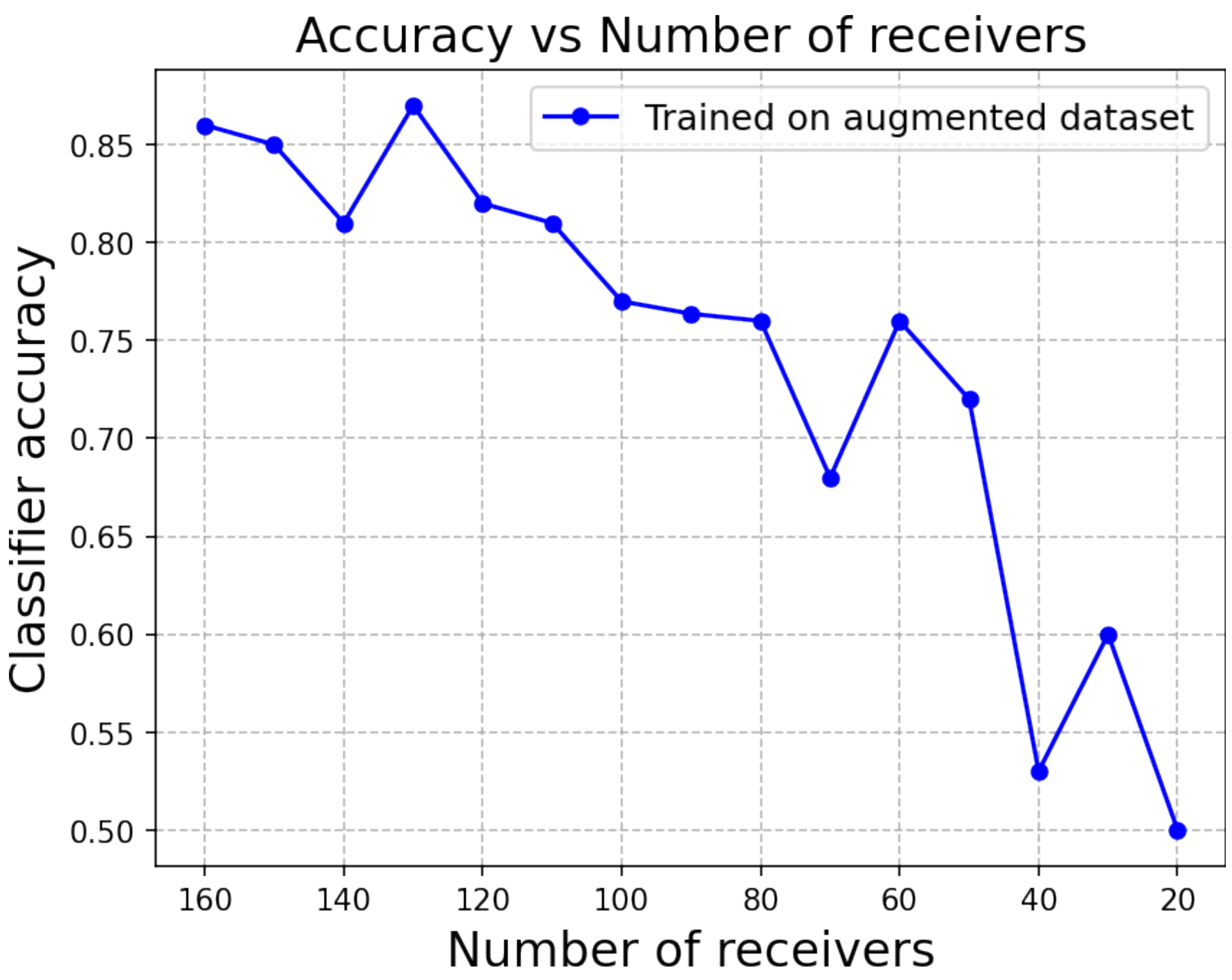

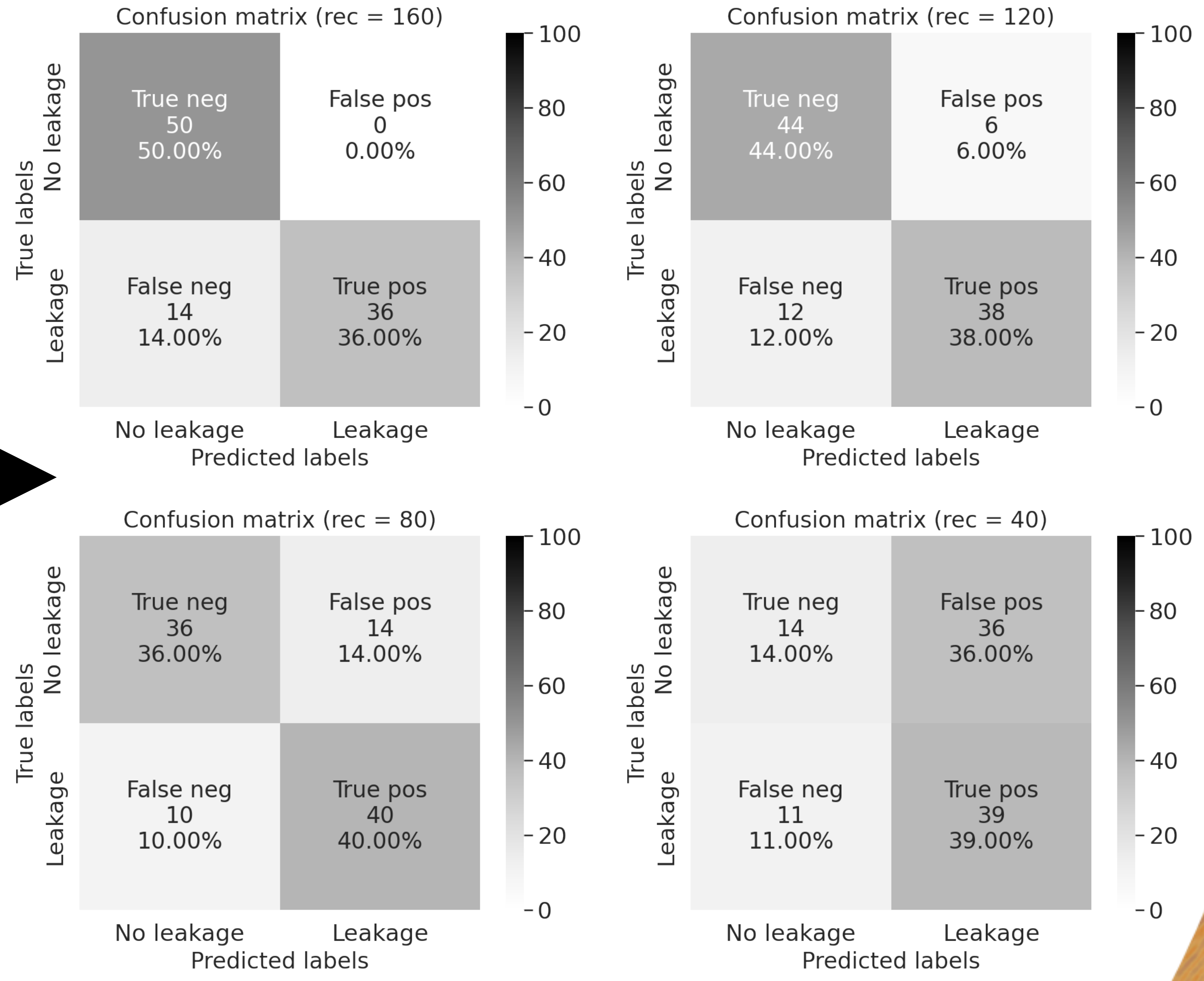

Huseyin Tuna Erdinc, Abhinav Prakash Gahlot, Mathias Louboutin, and Felix J. Herrmann, "**Enhancing CO2 Leakage Detectability via Dataset Augmentation**". 2023

SLIM ML4Seismic

Results

after data augmentation

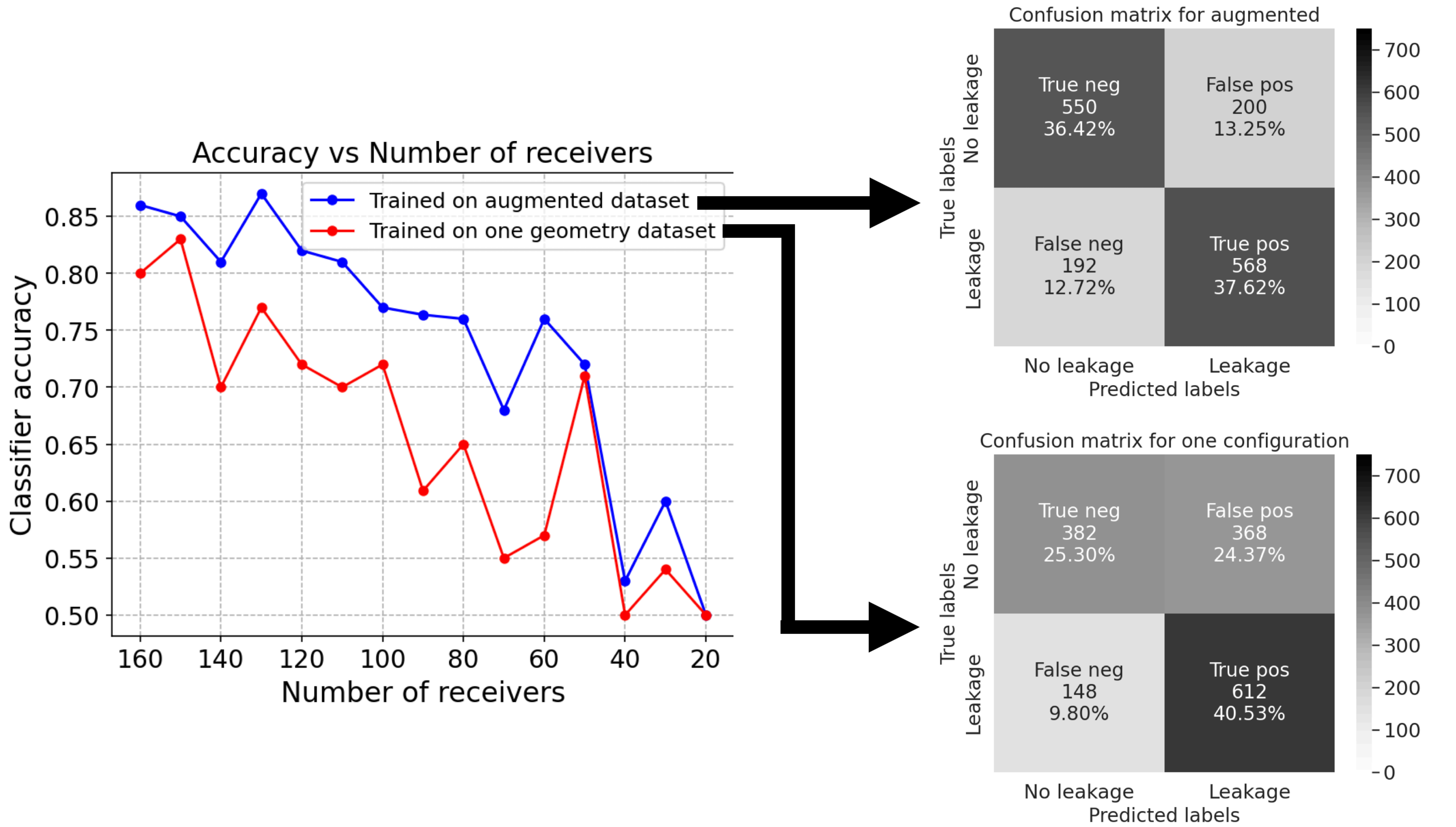

SLIM
ML4Seismic

Permeability inversion from time-lapse seismic data

Mathias Louboutin, Ziyi Yin, Rafael Orozco, Thomas J. Grady II, Ali Siahkoohi, Gabrio Rizzuti, Philipp A. Witte, Olav Møyner, Gerard J. Gorman, and Felix J. Herrmann, "**Learned multiphysics inversion with differentiable programming and machine learning**". 2023

End-to-end inversion
permeability

Mathias Louboutin, Ziyi Yin, Rafael Orozco, Thomas J. Grady II, Ali Siahkoohi, Gabrio Rizzuti, Philipp A. Witte, Olav Møyner, Gerard J. Gorman, and Felix J. Herrmann, "**Learned multiphysics inversion with differentiable programming and machine learning**". 2023

SLIM ML4Seismic

permeability $\mathbf{K}$

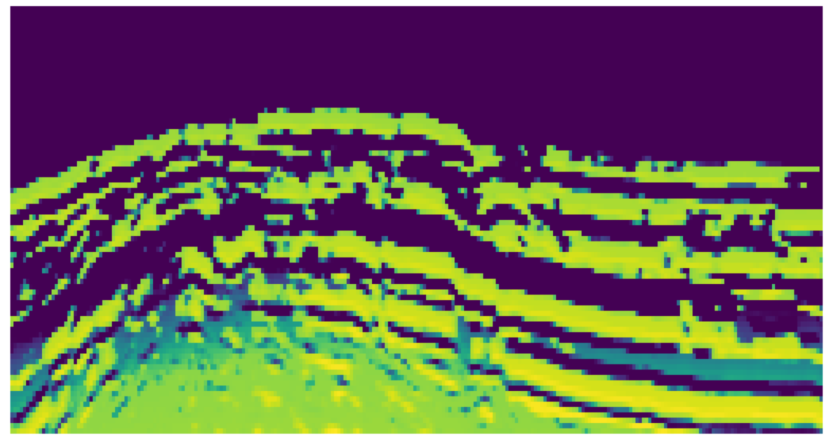

$\xrightarrow{\mathscr{S}}$ **fluid-flow physics**

CO_2 concentration $\mathbf{c}$

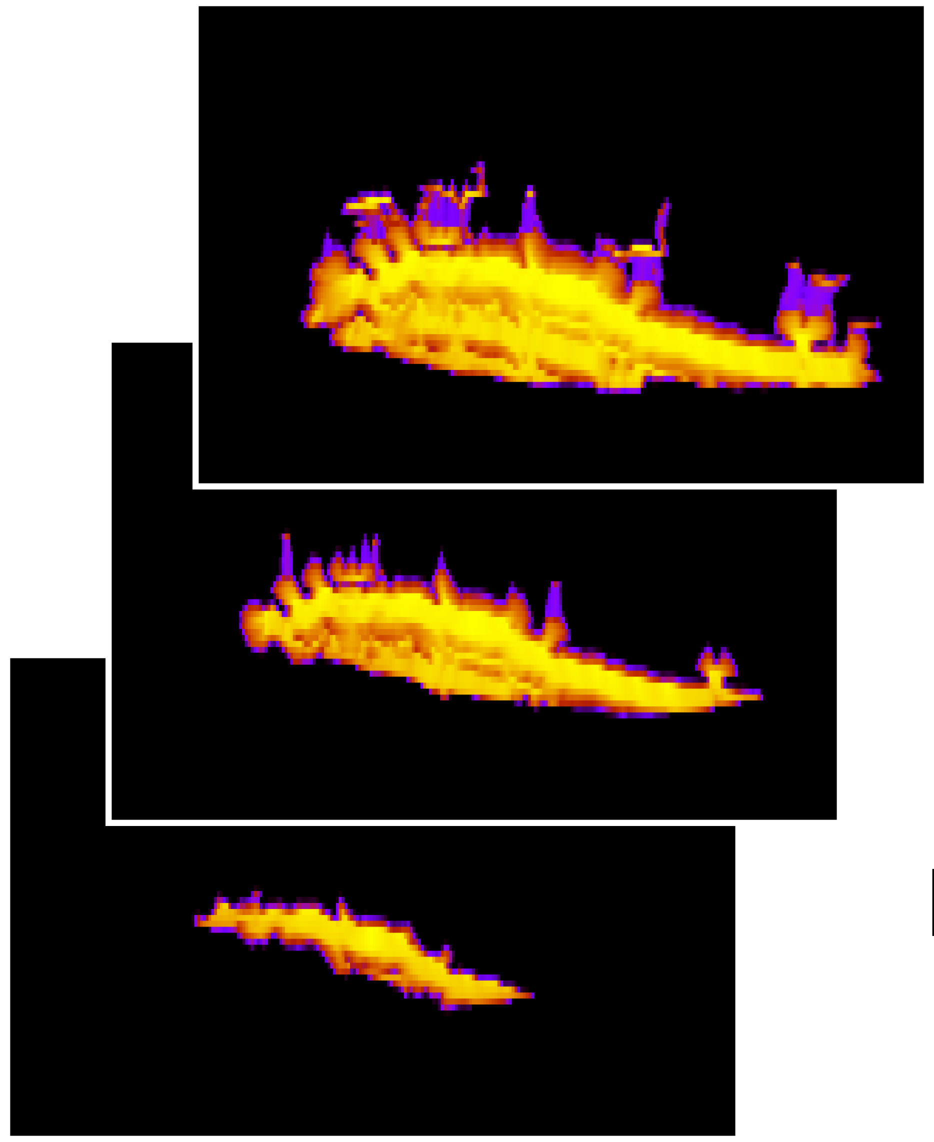

$\xrightarrow{\mathscr{R}}$ **rock physics**

wavespeed $\mathbf{v}$

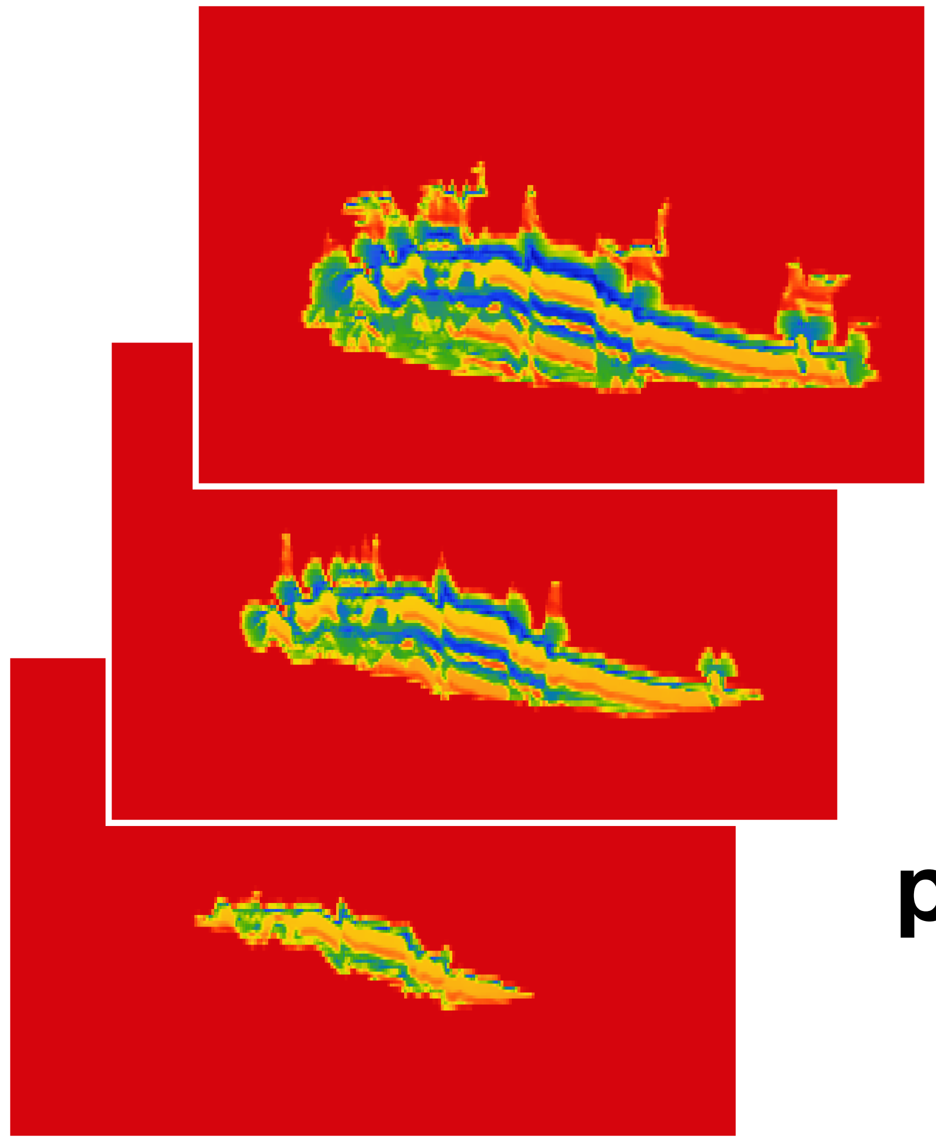

$\xrightarrow{\mathscr{F}}$ **wave physics**

time-lapse data $\mathbf{d}$

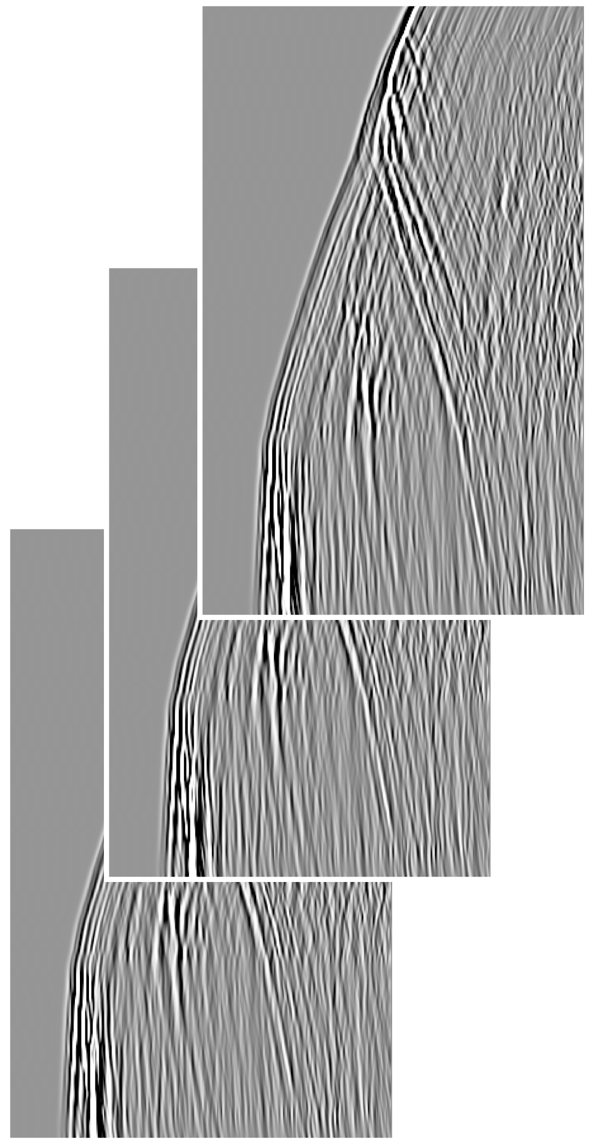

$$\underset{\mathbf{K}}{\text{minimize}} \quad \|\mathscr{F} \circ \mathscr{R} \circ \mathscr{S}(\mathbf{K}) - \mathbf{d}\|_2^2$$

CO_2 plume
predictions & forecast

SLIM
ML4Seismic

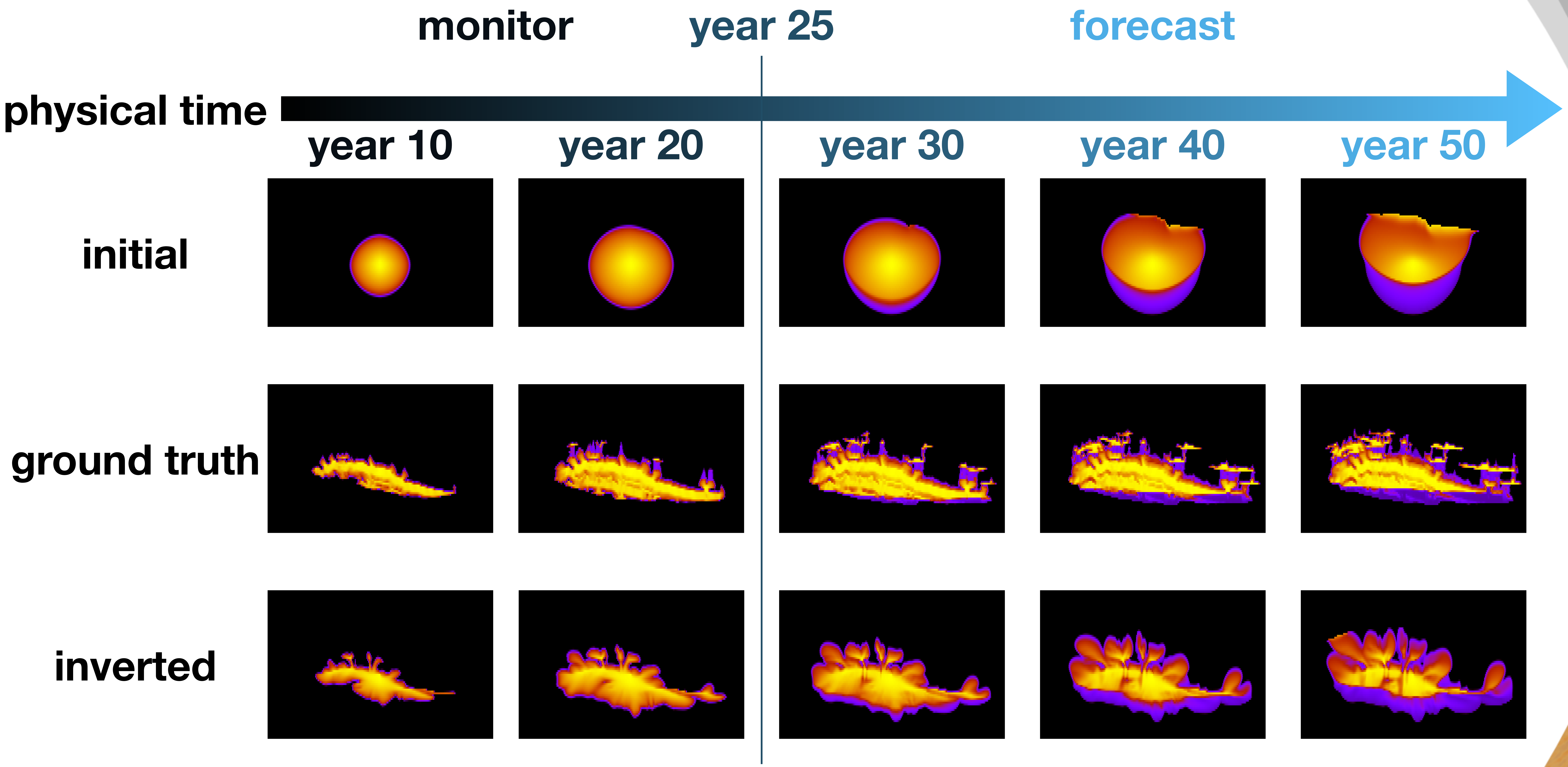

Permeability inversion

Mathias Louboutin, Ziyi Yin, Rafael Orozco, Thomas J. Grady II, Ali Siahkoohi, Gabrio Rizzuti, Philipp A. Witte, Olav Møyner, Gerard J. Gorman, and Felix J. Herrmann, "**Learned multiphysics inversion with differentiable programming and machine learning**". 2023

SLIM
ML4Seismic

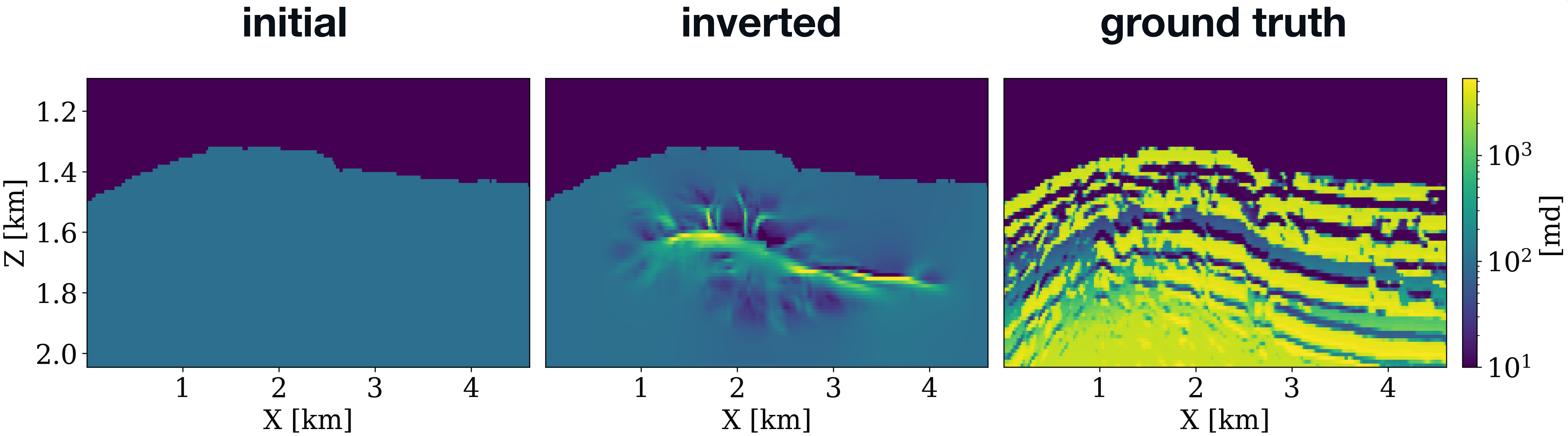

Julia packages can be found on the SLIM GitHub page (https://github.com/slimgroup).

SLIM ML4Seismic

Acknowledgements

This research was carried out with the support of Georgia Research Alliance and partners of the ML4Seismic Center.

Thank the Diamond sponsors (Equinor ASA, Microsoft Corporation, Occidental Petroleum) and Platinum sponsors (Chevron Corporation, ExxonMobil Corporation, Shell plc, S&P Global Inc) for their support.

This work was supported in part by the US National Science Foundation grant OAC 2203821 and the Department of Energy grant No. DE-SC0021515.

https://slim.gatech.edu/